Review

Bioenergetics and anaerobic respiratory chains of aceticlastic methanogens ☆

Cornelia Welte [a,b], Uwe Deppenmeier [a,*]

[a] Institute of Microbiology and Biotechnology, University of Bonn, Meckenheimer Allee 168, 53115 Bonn, Germany
[b] Department of Microbiology, IWWR, Radboud University Nijmegen, Heyendaalseweg 135, 6525 AJ Nijmegen, The Netherlands

ABSTRACT

Methane-forming archaea are strictly anaerobic microbes and are essential for global carbon fluxes since they perform the terminal step in breakdown of organic matter in the absence of oxygen. Major part of methane produced in nature derives from the methyl group of acetate. Only members of the genera *Methanosarcina* and *Methanosaeta* are able to use this substrate for methane formation and growth. Since the free energy change coupled to methanogenesis from acetate is only -36 kJ/mol CH$_4$, aceticlastic methanogens developed efficient energy-conserving systems to handle this thermodynamic limitation. The membrane bound electron transport system of aceticlastic methanogens is a complex branched respiratory chain that can accept electrons from hydrogen, reduced coenzyme F$_{420}$ or reduced ferredoxin. The terminal electron acceptor of this anaerobic respiration is a mixed disulfide composed of coenzyme M and coenzyme B. Reduced ferredoxin has an important function under aceticlastic growth conditions and novel and well-established membrane complexes oxidizing ferredoxin will be discussed in depth. Membrane bound electron transport is connected to energy conservation by proton or sodium ion translocating enzymes (F$_{420}$H$_2$ dehydrogenase, Rnf complex, Ech hydrogenase, methanophenazine-reducing hydrogenase and heterodisulfide reductase). The resulting electrochemical ion gradient constitutes the driving force for adenosine triphosphate synthesis. Methanogenesis, electron transport, and the structure of key enzymes are discussed in this review leading to a concept of how aceticlastic methanogens make a living. This article is part of a Special Issue entitled: 18th European Bioenergetic Conference.

© 2013 Elsevier B.V. All rights reserved.

1. Introduction

Methane producing microorganisms belong to the domain of the *Archaea* and are of great interest because of their important ecological function and their unique biochemical features. Methanogens are strictly anaerobic organisms and are found in anoxic environments such as fresh water sediments, tundra areas, swamps and the intestinal tract of ruminants and termites as well as in man-made environments such as rice fields, anaerobic digesters of sewage plants and biogas plants [1,2]. The formation of methane belongs to the most important global bioelement fluxes because it marks the end of the anaerobic food chain for the recycling of carbon components from organic matter [3]. In this process biopolymers are hydrolyzed to mainly sugars, amino acids, purines, pyrimidines, fatty acids and glycerol. Fermentative bacteria convert these organic compounds to simple carbonic acids (e.g. propionate, butyrate and acetate), alcohols (e.g. ethanol, propanol and butanol) and some other compounds (e.g. H$_2$, CO$_2$ and ketones). These products are used as substrates by syntrophic bacteria, which

form acetate and H$_2$ + CO$_2$ [4–6]. These end products of fermentative degradation are then converted to methane by methanogenic archaea [7]. The major part of the methane released from anaerobic habitats is oxidized by aerobic bacteria. However, billions of metric tons of CH$_4$ per year escape into the atmosphere where methane contributes to global warming since it is a 20 times more potent greenhouse gas than carbon dioxide [8,9]. In addition, methanogens are involved in the formation of the so-called methane hydrates [10] which may represent one of the largest sources of hydrocarbon on earth [11]. These methane-trapping, water-ice-like structures are naturally formed at high pressures and low temperatures, and are found within ocean continental slopes and in permafrost regions. There are indications that climatic changes in the past were based on large releases of methane into the atmosphere. Therefore, concerns have arisen about the possible impacts of a temperature increase on the present deposits of methane hydrates [12]. On the other hand methanogens are an integral part of biogas reactors and essential for the production of the combustible gas methane that is a renewable energy source, and is used for the generation of electricity and heat. In Germany alone more than 7000 biogas plant were built until 2011 producing about 3000 MW of electric power, a capacity that is comparable to the performance of about three atomic power plants [13]. Moreover, methane-enriched and purified biogas can be fed into gas distribution

networks and can replace natural gas as a feedstock for producing chemicals and materials. Hence, biogas production has a huge economical value and is of interest in order to substitute fossil fuels.

2. Acetate converting methanogens

Methanogenic archaea are divided into seven taxonomic orders each of which is as distantly related to the other as humans are to slime moulds. Species of the orders Methanobacteriales, Methanococcales, Methanomicrobiales, Methanocellales, Methanopyrales and Methanoplasmatales are obligate hydrogenotrophic organisms and use $H_2 + CO_2$ (or in some cases H_2 + methanol) as substrate [14]. In addition, most of them can oxidize formate that is converted to $H_2 + CO_2$ and then used for methanogenesis. However, the obligate hydrogenotrophic methanogens are not able to utilize acetate [15] and are therefore not discussed in this review (for a detailed description of these methanogens see [9,16–19]). The major part of methane in nature derives from the methyl group of acetate but only two genera, namely *Methanosarcina* and *Methanosaeta*, have been described to use this substrate for methanogenesis and growth [20].

Members of the genus *Methanosarcina* have the broadest substrate spectrum of all methanogens and use acetate, methanol and other methylated C_1 compounds such as methylamines and methylated thiols for methane formation. Some of them are also able to utilize $H_2 + CO_2$ [21]. The species reveal a number of distinct morphological forms including single cells and sarcina packages, as well as multicellular packets and lamina [22]. Single cells are coccoid and are covered by S-layer proteins that are sometimes overlaid by sheets of heteropolysaccharides. This structure is called methanochondroitin and closely resembles eukaryotic chondroitin [22]. Furthermore, *Methanosarcina* species are unsurpassed among methanogens in terms of metabolic, physiological and environmental versatility. These capabilities are reflected in the genomes of *Methanosarcina* (*Ms.*) *acetivorans* (5.7 Mbp), *Ms. barkeri* (4.8 Mbp) and *Ms. mazei* (4.1 Mbp) that are more than twice as large as the genomes of obligate hydrogenotrophic methanogens [23–25]. The genomes reveal extensive genetic diversity and redundancy underlining the ability of *Methanosarcina* strains to adapt to various environmental conditions. In addition, the genomes indicate the potential for entirely unexpected metabolic capabilities. One of the most interesting features is the fact that *Methanosarcina* species obviously acquired hundreds of eubacterial genes [26], among them many which encode subunits of key enzymes of the energy conserving machinery.

Species of the genus *Methanosaeta* form rod-shaped cells and are normally combined end to end in long filaments, surrounded by a sheath-like structure [27]. While *Methanosarcina* species are metabolically versatile, members of the genus *Methanosaeta* are specialized on acetate degradation. A minimal concentration of only 7–70 μM is needed for growth indicating a high affinity to this substrate [28,29]. From the genome sequences of *Methanosaeta* (*Mt.*) *thermophila* (1.9 Mbp) [30], *Mt. harundinacea* (2.6 Mbp) [31] and *Mt. concilii* (3.0 Mbp) [32] and from pathway reconstruction [30,33] it is evident that the key enzymes of the core processes of methane formation from acetate are similar to the ones found in *Methanosarcina* species.

3. Biochemistry of methanogenesis

In this review we will focus on methane formation from acetate and will only briefly present data on methanogenesis from other substrates. For further reading we refer to excellent reviews that have been published in the last five years [9,16,20,34–36].

3.1. Methanogenic cofactors

Several unusual coenzymes and prosthetic groups participate in methanogenesis of aceticlastic methanogens [37], which are

referred to as methanofuran (MFR), tetrahydrosarcinapterin (H_4SPT), 2-mercaptoethanesulfonate (coenzyme M or HS-CoM), *N*-7-mercaptoheptanoyl-L-threonine phosphate (coenzyme B or HS-CoB), coenzyme F_{420} (F_{420}), coenzyme F_{430} and methanophenazine (Mph) (Fig. 1). MFR und H_4SPT are carriers of C_1-fragments between formyl and methyl oxidation levels in the process of methanogenesis from $H_2 + CO_2$ and methylated C_1 compounds. HS-CoM is a ubiquitous methyl group carrier in the pathway of methanogenesis. The methylated form, CH_3-S-CoM, is the substrate for the methyl-CoM reductase that catalyzes the terminal step of methanogenesis. This enzyme contains another unusual and unique methanogenic cofactor called coenzyme F_{430} [38–40]. It is made of a reduced tetrapyrrole ring system that coordinates a nickel ion [41,42]. HS-CoM, F_{420} and Mph function as electron carriers in methanogenesis (Fig. 1) [19,37]. F_{420} is a deazaflavine derivative with a midpoint potential of −360 mV and is a central electron carrier in the cytoplasm of methanogens [43]. HS-CoB is used as electron donor in the process of methane formation from CH_3-S-CoM as catalyzed by the methyl-CoM reductase (Fig. 2) [44,45]. The last unusual cofactor discovered in *Methanosarcina* species was Mph (Fig. 1). It functions as electron carrier within the cytoplasmic membrane with a mid-point potential of −165 mV that replaces quinones that are not present in methanogens. This cofactor represents a 2-hydroxyphenazine derivative that is linked via an ether bridge to a pentaisoprenoid side chain [46–48].
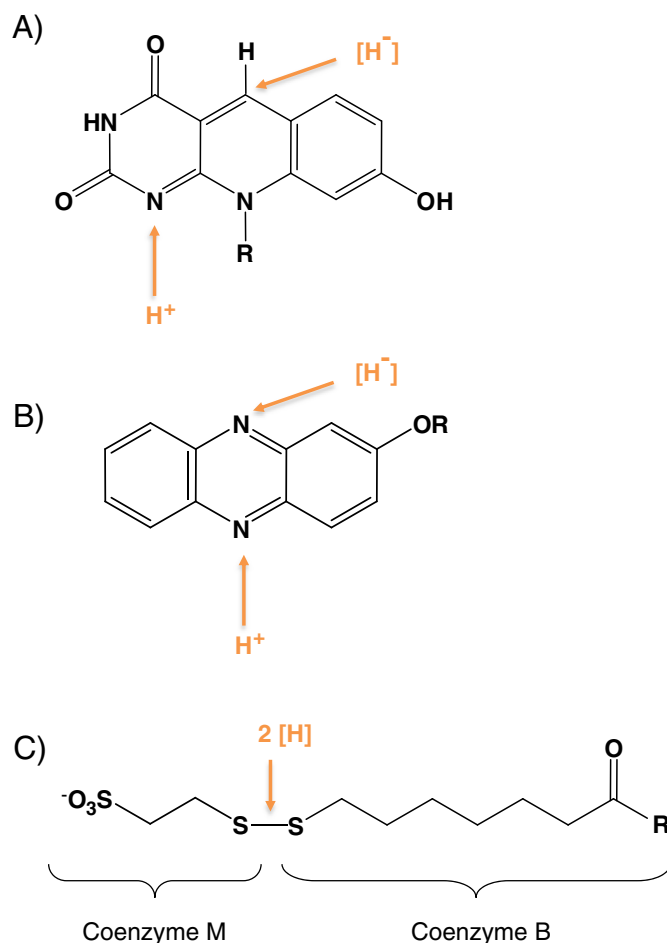
Fig. 1. Chemical structure of electron carriers involved in methanogenesis. (A) F_{420}, (B) Mph, (C) CoM-S-S-CoB (the parts of the molecule representing coenzyme M and B are indicated). Only the oxidized form of the reactive part of the cofactors is shown. The positions for reduction are indicated in red.

3.2. Methane formation from acetate

As mentioned above the major part of methane produced in nature derives from the methyl group of acetate. So far only two genera, *Methanosarcina* and *Methanosaeta*, were found to use this substrate for methane formation and growth. At first glance the conversion of acetic acid to methane and carbon dioxide seems simple:

$$CH_3-COOH \rightarrow CH_4 + CO_2. \hspace{3cm} (1)$$

However, the biochemistry of this process is complex and involves many interesting enzymes (Fig. 2). In *Methanosarcina* strains the so-called aceticlastic pathway of methanogenesis starts with the activation of the carboxyl group of acetate by ATP-dependent phosphorylation, catalyzed by an acetate kinase. Then a phosphotransacetylase converts the resulting acetyl-phosphate to acetyl-CoA [1,49]. In obligate aceticlastic *Methanosaeta* species activation of acetate is performed by an acetyl-CoA synthetase forming acetyl-CoA, AMP and pyrophosphate (PP_i) from acetate, HS-CoA and ATP [28,30,50]. PP_i can be hydrolyzed by a pyrophosphatase to drive the reaction [28,50] (Fig. 2). One consequence of these basic differences is that the minimum threshold concentration for acetate is much lower in *Methanosaeta* than in *Methanosarcina* species. At high acetate concentrations the faster growing *Methanosarcina* species out-compete *Methanosaeta* species, but at acetate concentrations below 1 mM members of the genus *Methanosaeta* prevail [29,50]. The acetyl-CoA synthetase has been purified from *Mt. concilii* and *Mt. thermophila* [28,51,52] and showed activities of 55 and 26 U/mg protein and low K_m values of 0.86 mM

and 0.4 mM, respectively. In contrast, the K_m value of the acetate kinase in *Methanosarcina* species can be as high as 48 mM [53]. Hence, the high affinity of the acetyl-CoA synthetase to acetate could be the reason for the low threshold concentration in *Mt. thermophila*. The key reaction of aceticlastic methanogenesis is the cleavage of acetyl-CoA into its methyl and carbonyl moiety by the action of a CO dehydrogenase/acetyl-CoA synthase (Fig. 2). The enzyme of *Methanosarcina* species is composed of a five-subunit complex (CdhABCDE) [54–57]. It has been shown that CdhC is responsible for the cleavage of the C-S bond and transfers the acetyl moiety to the so-called cluster A composed of a binuclear Ni–Ni-site and a [4Fe4S] cluster. After cleavage of the C–C bond the methyl group is transferred to the corrinoid containing subcomplex CdhDE, which in turn transfers the methyl group to the methanogenic cofactor H_4SPT. The CO moiety is then oxidized to CO_2 by the subcomplex CdhAE (Fig. 2). The electrons are used for ferredoxin (Fd) reduction (for details please see James G. Ferry's review [1]). The critical factor for electron transfer from enzyme-bound CO to Fd is the active site C composed of an $NiFe_3S_4$ cluster bridged to an exogeneous Fe atom [58]. It is postulated that the removal of the CO_2, produced in the course of the aceticlastic pathway, optimizes the thermodynamic efficiency of growth. The conversion of CO_2 to HCO_3^- is performed by an extracellular carbonic anhydrase [1].

In the subsequent reaction the methyl-group bound to H_4SPT is transferred to HS-CoM (Fig. 2). This exergonic reaction is catalyzed by a membrane bound methyltransferase (MtrA-H) that couples methyl-group transfer to sodium ion extrusion across the cytoplasmic membrane resulting in the generation of an electrochemical sodium ion gradient [59–61]. Subsequently, methyl-S-CoM is reduced to
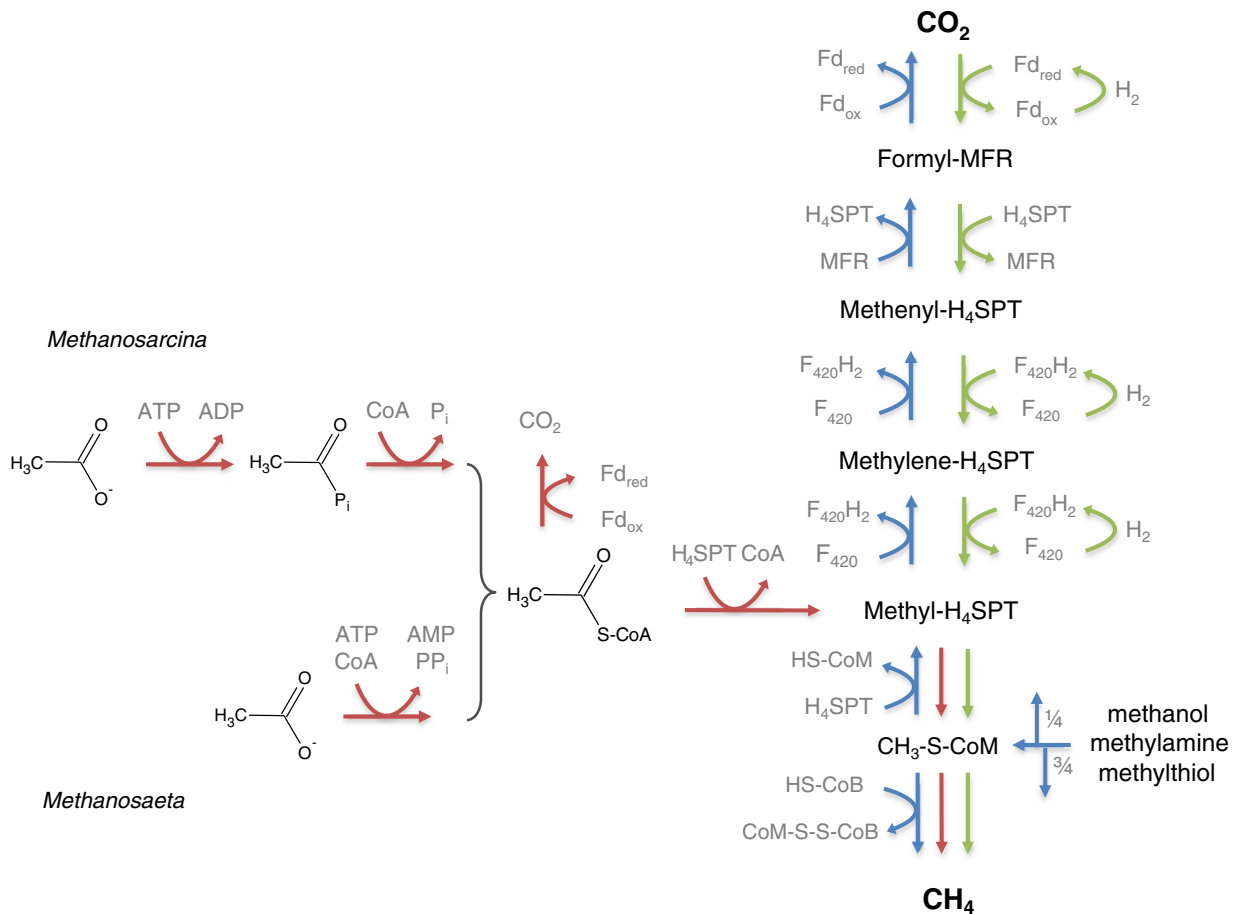

Fig. 2. Pathways of methanogenesis. Carbon fluxes through the three pathways of methanogenesis in *Methanosarcina* and *Methanosaeta* strains. Red arrows indicates aceticlastic methanogenesis with the different acetate activation mechanisms in *Methanosarcina* and *Methanosaeta*. Blue arrows indicate reactions of methylotrophic methanogens. Green arrows indicate the pathway of hydrogenotrophic methanogenesis by a subgroup of *Methanosarcina* strains, e.g. *Ms. mazei*.

methane, catalyzed by the methyl-CoM reductase. Electrons derive from coenzyme B, causing the formation of a mixed disulfide from coenzyme M and coenzyme B which is called heterodisulfide (CoM-S-S-CoB) [62,63]. CoM-S-S-CoB functions as terminal electron acceptor of an anaerobic respiratory chain that is described in Sections 4.2 and 4.3.

### 3.3. Methanogenesis from $H_2 + CO_2$ and methylated compounds

Members of the family Methanosarcinaceae can grow on methylated C_1 compounds (e.g. methanol and methylamines) in the absence of H_2 (Fig. 2). This pathway is referred to as methylotrophic methanogenesis.

$$4\ CH_3OH \rightarrow 3\ CH_4 + 1\ CO_2 + 2\ H_2O \qquad (2)$$

The methyl groups are channelled into the central pathway by substrate-specific soluble methyltransferases that catalyze the transfer of the methyl group to HS-CoM [64]. To generate reducing equivalents for methane production, parts of the methyl groups are oxidized. In general, three out of four methyl groups are reduced to methane and one methyl group is oxidized to CO_2. In the oxidative branch of the pathway the methyl group is transferred from methyl-CoM to H_4SPT (Fig. 2). This endergonic reaction is driven by a sodium ion potential and catalyzed by the membrane bound methyl transferase MTR [59] that couples the transfer reaction with the vectorial import of two Na^+ ions across the membrane into the cytoplasm. The methyl group in H_4SPT is then stepwisely oxidized forming formyl-H_4SPT with the reducing equivalents being used for F_{420} reduction. After transfer of the formyl group to MFR the formyl-MFR dehydrogenase catalyzes the oxidation to CO_2 and MFR. The electrons are transferred to Fd forming reduced Fd (Fd_{red}) [65]. In summary, the oxidation of the cofactor bound methyl moiety is the exact reversal of the CO_2-reducing pathway as described above and provides reduced cofactors ($2\ F_{420}H_2$ and Fd_{red}) in the absence of H_2. In the reductive branch of the pathway three out of four methyl-S-CoM molecules are reduced by the HS-CoB-dependent methyl-S-CoM reductase reaction leading to the formation of 3 CH_4 and 3 CoM-S-S-CoB (Fig. 2). Further conversion of CoM-S-S-CoB is described in Section 4.

In Methanosarcina species, hydrogenotrophic methanogenesis from $H_2 + CO_2$ starts with the H_2^- and MFR-dependent reduction of CO_2 to formyl-MFR (Fig. 2). The reaction is catalyzed by a formyl-MFR dehydrogenase and electrons are delivered by low potential Fd, that is reduced by the Ech hydrogenase at the expense of the proton gradient (Section 4.3) [35]. In Methanosarcina species the formyl group is then transferred to H_4SPT and the resulting formyl-H_4SPT is stepwisely reduced to methyl-H_4SPT. The electrons derive from reduced F_{420} ($F_{420}H_2$) that is produced by the F_{420}-reducing hydrogenase (Frh) [66]. The reactions for methyl group transfer and reduction are the same as described for the aceticlastic pathway of methanogenesis (Fig. 2) (Section 3.2). At this point it is important to mention that the mechanisms of CO_2 reduction in hydrogenotrophic methanogens and the mode of energy conservation is different from Methanosarcina species and other members of the order Methanosarcinales [34]. The process of redox driven ion translocation across the membrane in members of the order Methanosarcinales is based on cytochromes. This group of organisms will be discussed in detail in this review. In contrast, obligate hydrogenotrophic methanogens lack cytochromes and cannot couple membrane bound electron transfer reactions with the extrusion of protons or sodium ions. However, they are forced to produce reduced ferredoxin with a midpoint potential of about -500 mV to catalyze the first step of methanogenesis, the reduction of CO_2 to formyl-MFR. This problem is solved by a cytoplasmic enzyme complex that couples the exergonic process of H_2-dependent CoM-S-S-CoB reduction to the endergonic H_2-dependent reduction of Fd. As the electrons derived from hydrogen oxidation are used for one exergonic (CoM-S-S-CoB) and one endergonic (Fd) reduction reaction, this process is called electron bifurcation. Electron bifurcation was first described for the

butyryl-CoA dehydrogenase/Etf complex from Clostridium kluyveri [67] and later proposed by Thauer et al. [34] for the hydrogenase/heterodisulfide reductase complex (MvhAGD/HdrABC) from methanogenic archaea. Subsequently, this was confirmed by purification and characterisation of the enzyme from Methanothermobacter marburgensis [34,68]. For Methanococcus maripaludis, a central role for electron bifurcation in methanogenesis was also detected [69,70]. Although this process allows obligate hydrogenotrophic methanogens to circumvent the dissipation of an ion gradient to drive the endergonic reduction of Fd with H_2, no energy is conserved in this reaction. The only process that leads to ion translocation in these organisms is the transfer of sodium ions during transfer of the methyl group from H_4MPT (close homologue of H_4SPT) to HS-CoM as catalyzed by the membrane bound methyltransferase Mtr (Section 3.2). This electrochemical sodium ion gradient is subsequently used for ATP synthesis.

$$CH_3-H_4MPT + CoM-SH \rightarrow CH_3-S-CoM + H_4MPT \qquad (3)$$
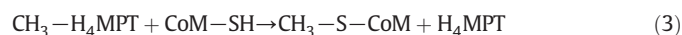
The electrochemical sodium ion gradient generated by methyl group transfer is also found in cytochrome-containing methanogens during growth on H_2/CO_2 and acetate but these organisms have many more opportunities to generate primary ion gradients as will be discussed in the next sections.

4. Reactions and compounds of the electron transport chain of aceticlastic methanogens

4.1. Membrane bound electron transport and energy conservation

Aceticlastic methanogens must possess efficient energy-conserving systems to cope with thermodynamic limitation because methane formation from acetate is coupled to a change of free energy of only -36 kJ/mol CH_4. As mentioned above, one or even two ATP molecules are spent for acetyl-CoA formation in the aceticlastic pathway of methanogenesis. However, it is obvious that there is no site for ATP regeneration by substrate level phosphorylation. Therefore, it is apparent that ATP synthesis is accomplished by the interaction of ion translocating enzymes and ATP synthases. Na^+ extrusion by methyl-group transfer as catalyzed by the membrane bound methyltransferase Mtr [59–61,71] has already been mentioned as one ion translocating mechanism. The ratio of sodium ion translocation per methyl group transfer is about 2, which fits to the thermodynamics of this reaction ($\Delta G^{0\prime} = -29$ kJ/mol) [72]. The other aspect of energy conservation concerns the formation of heterodisulfide, which marks the end of the processes leading to methane formation (Fig. 2). In recent years it became evident that the reduction of CoM-S-S-CoB and the oxidation of reduced cofactors (Fd_{red}, $F_{420}H_2$ and H_2) are catalyzed by membrane bound electron transport system in Methanosarcina species that couple the redox reaction with the translocation of protons or sodium ions (Fig. 3) [35,73]. In Methanosaeta species the respiratory chain is simpler and only Fd_{red} dependent reduction of the heterodisulfide was observed [33] (Section 6). Methanogens are the only microorganisms known to produce two primary ion gradients, $\Delta\tilde{\mu}_{Na+}$ and $\Delta\tilde{\mu}_{H+}$, at the same time [74]. This finding raised the question whether the A_1A_O ATP synthase found in methanogens [75–77] uses both ions for ATP synthesis or whether Na^+/H^+ antiporters convert one gradient into the other. Recent studies on the A_1A_O ATP synthase of Ms. acetivorans finally provided the answer. With the help of ATP hydrolysis assays and by analyzing ion transport in inverted membrane vesicles it was demonstrated that the A_1A_O ATP synthase from Ms. acetivorans uses both H^+ and Na^+ for energetic coupling leading to ATP synthesis [78]. The Ms. acetivorans Na^+/H^+ antiporter Mrp is hypothesized to be used for optimization of the thermodynamic efficiency of the ATP synthase by adjusting the ratio of $\Delta\tilde{\mu}_{Na+}$ and $\Delta\tilde{\mu}_{H+}$ [79]. The actual values of electrochemical ion gradients have been measured only in a few bacteria and archaea. For Ms. mazei and Ms. barkeri, $\Delta\tilde{\mu}_{H+}/F$ was in the
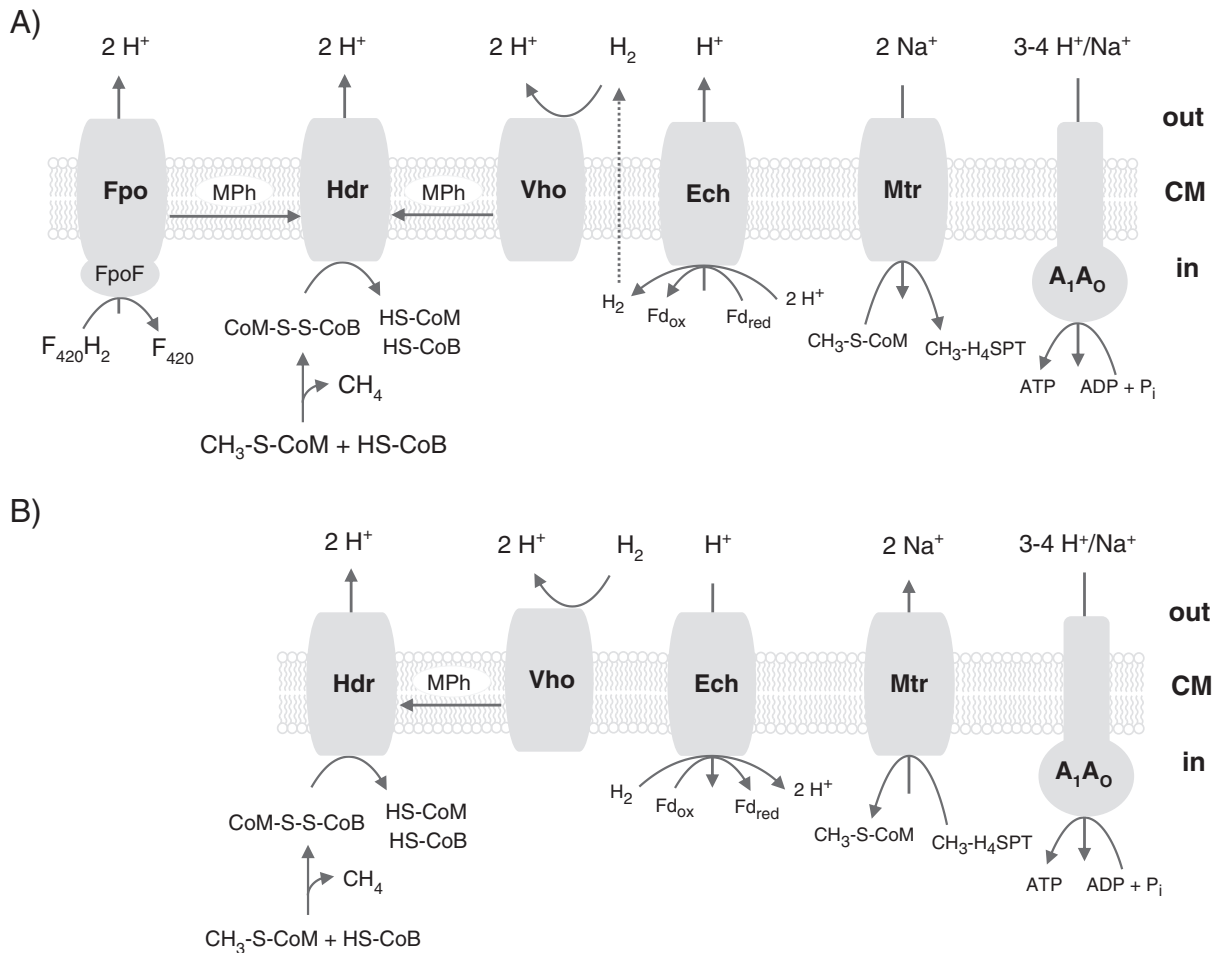
Fig. 3. All ion-translocating enzymes of *Ms. mazei* in action. (A) methylotrophic methanogenesis, (B) hydrogenotrophic methanogenesis. The scheme gives an overview of ion translocation events and does not indicate the mechanism of ion translocation. Vho, Mph-reducing hydrogenase; Ech, Ech hydrogenase; Hdr, heterodisulfide reductase. Fpo, $F_{420}H_2$ dehydrogenase; FpoF, input module of the Fpo complex; Mtr, methyl-H_4SPT–coenzyme M methyltransferase; A_1A_O, ATP synthase; CM, cytoplasmic membrane. Please note that in *Ms. acetivorans* Vho and Ech are replaced by the Na^+-translocating Rnf complex.

range of -0.12 to -0.15 V [80,81]. Together with the chemical Na^+ gradient (about -30 mV) [82] the value for the total electrochemical ion potential $\Delta\tilde{\mu}_{ion}/F$) adds up to -0.15 to -0.18 V. Synthesis of ATP as catalyzed by the ATP synthase is a highly endergonic reaction and depends on the cellular concentrations of ATP, ADP, and P_i. This correlation is described by the phosphorylation potential (ΔG_p) and has been determined only for the hydrogenotrophic methanogen *Methanococcus voltae* ($\Delta G_p = 43.3$ kJ/mol) and the aceticlastic methanogen *Methanosaeta concilii* ($\Delta G_p = 45$ kJ/mol). The number of ions needed by the ATP synthase to phosphorylate ADP is given by Eq. (4).

$$\Delta G_p = -n \times F \times \Delta\tilde{\mu}_{ion} \text{ (with } \Delta\tilde{\mu}_{ion} = \text{sum of } \Delta\tilde{\mu}_{Na^+} \text{ and } \Delta\tilde{\mu}_{H^+}) \qquad (4)$$

Taking together these values and considering Eq. (4) we can conclude that the methanogenic ATP synthase needs 3–4 translocated ions (H^+ or Na^+) to synthesize one molecule of ATP. As indicated above this value is highly dependent on the actual electrochemical ion potential and on the concentration of ATP, ADP and P_i within the cell and may vary depending on growth conditions. The reactions and the components involved in the energy transducing systems will be described in the next sections.

4.2. Electron transport chain using reduced F_{420} or molecular hydrogen as electron donors

To describe the processes of energy conservation of aceticlastic methanogens it is necessary to have a look at electron transport

processes that take place during growth on $H_2 + CO_2$ and methylated C_1 compounds. As indicated above, the hydrogenotrophic pathway of methanogenesis produces CoM-S-S-CoB that contains a disulfide bridge and is used as terminal electron acceptor. Indeed, it has been shown that membrane preparations of *Ms. mazei* catalyze a H_2-dependent CoM-S-S-CoB reduction, whereas methyl-CoM or other disulfide compounds do not serve as electron acceptors [83]. The electron transport system is referred to as H_2:heterodisulfide oxidoreductase and is involved in methanogenesis from $H_2 + CO_2$.

$$H_2 + CoM-S-S-CoB \rightarrow HS-CoM + HS-CoB \qquad (5)$$
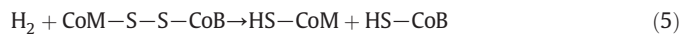
The redox reactions are catalyzed by two membrane bound enzymes (Fig. 3A/B): i) the Mph-reducing hydrogenase (Vho) (Section 5.1) oxidizes H_2 and transfers the electrons to the Mph pool within the cytoplasmic membrane. Two protons are released at the extracellular side when the H_2 molecule is oxidized, and Mph takes up two protons in the course of reduction, so a vectorial proton translocation with the stoichiometry of $2H^+/2e^-$ can be observed [84]. ii) The heterodisulfide reductase catalyzes the final step in the anaerobic respiratory chain of *Methanosarcina* species. This reaction involves the two-electron reduction of CoM-S-S-CoB to the free thiols HS-CoB and HS-CoM. Electrons are provided by reduced Mph (Mph$_{red}$). This reaction is also coupled to a transfer of $2H^+/2e^-$ [84] (Fig. 3A/B).

Reduced F_{420} ($F_{420}H_2$) and CoM-S-S-CoB are formed in methylotrophic methanogens during methanogenesis from methanol and methylamines (Section 3.3, Fig. 2). A system referred to as

as F_{420}:heterodisulfide oxidoreductase oxidizes $F_{420}H_2$ at the expense of CoM-S-S-CoB reduction (Fig. 3B) [85,86] (an alternative pathway is presented in [87]).

$$CoM-S-S-CoB + F_{420}H_2 \rightarrow HS-CoM + HS-CoB + F_{420} \qquad (6)$$
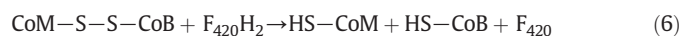
It has been shown that Mph is reduced by the membrane bound $F_{420}H_2$ dehydrogenase from *Ms. mazei* with $F_{420}H_2$ as electron donor (Section 5.3). In the course of the reaction $2H^+/2e^-$ are transferred across the cytoplasmic membrane. The resulting Mph_{red} acts as substrate for the heterodisulfide reductase which also transfers two protons in the course of CoM-S-S-CoB reduction (Section 4.1). Hence, the electron transport chain is composed of a $F_{420}H_2$ dehydrogenase and the heterodisulfide reductase connected by Mph (Fig. 3b). Similar to the H_2:heterodisulfide oxidoreductase, electron transport and H^+ translocation are strictly coupled, as indicated by stoichiometries of $4H^+/2e^-$ [85].

The ratios of proton translocation and electron transport fit well to the thermodynamic requirements. The midpoint potentials of the electron carriers under standard conditions are -414 mV for $H_2/2H^+$, -360 mV for $F_{420}H_2/F_{420}$ [43], -165 mV for Mph/Mph_{red} and -143 mV for CoM-S-S-CoB/HS-CoM + HS-CoB [48]. Taking into account the electrochemical proton potential Δp of -180 mV in *Ms. mazei* [35] the translocation of two protons is possible when H_2 or $F_{420}H_2$ are used for Mph reduction (Eq. (7)).

$$n = 2 \times 2\Delta E^0/\Delta p \qquad (7)$$

(with $\Delta E^{0\prime}$ = midpoint potential under standard conditions, Δp = electrochemical proton potential, n = number of ions translocated [88]).

The situation is different for the Mph_{red} dependent reduction of CoM-S-S-CoB because under standard conditions the reaction is only slightly exergonic (-4.2 kJ/mol). Therefore, it was assumed that proton translocation as catalyzed by the heterodisulfide reductase is indirectly connected to the highly exergonic reduction of methyl-CoM (-30 kJ/mol) [89]. The methyl-CoM reductase keeps the concentration of the substrate of the heterodisulfide reductase high (CoM-S-S-CoB) and of the products low (HS-CoM and HS-CoB). It thus shifts the reaction equilibrium in favour of the heterodisulfide reductase reaction. Therefore, it is tempting to speculate that the $\Delta G\prime$ value under cellular conditions is negative enough for the translocation of two protons [35].

4.3. Reduced ferredoxin as electron donor

During recent years it became evident that the above described electron transport systems have to be extended because additional enzymes participate in the respiratory chain of *Methanosarcina* species. The key element of the extended view is Fd that can function as electron acceptor or electron donor in membrane bound electron transport (Figs. 3–5).

As described above, Fd_{red} derives from the oxidation of the carbonyl group of acetyl-CoA in the aceticlastic pathway of methanogenesis [55]. During methylotrophic growth, Fd is reduced in the course of formyl-MFR oxidation [90–92] (Fig. 2). Interestingly, the pathway of the oxidation of Fd_{red} differs in members of the genus *Methanosarcina*. *Ms. mazei* and *Ms. barkeri* take advantage of the Ech hydrogenase (Section 5.1.2) and the electrons are transferred to protons to form molecular hydrogen [92–95] (Fig. 4A). In the hydrogenase-negative strains *Ms. acetivorans* and *Ms. thermophila* the reaction is catalyzed by the recently described Rnf complex [96,97] (Section 5.2 and Fig. 4B).

Since the discovery of the Ech hydrogenase it was suggested that the enzyme could contribute to the electrochemical ion gradient [93] because of homologies to certain subunits of complex I of the respiratory chain of bacteria and eukaryotes. Furthermore, the idea of an energy conservation potential of the Ech hydrogenase was based on growth data, experiments on resting cells and cell suspensions [93,94,98,99].

Many scientists took up the hypothesis but direct experimental evidence for a redox-driven ion transfer as catalyzed by the Ech hydrogenase was lacking. In 2010, it was finally demonstrated that the Ech hydrogenase indeed translocates protons in the course of the oxidation of Fd_{red} (Figs. 3A and 4A) [95]. The experiments clearly showed that membrane vesicles of *Ms. mazei* couple the oxidation of Fd_{red} to hydrogen evolution and ATP formation. Furthermore, the addition of a protonophore resulted in a complete inhibition of ATP formation without inhibiting hydrogen production by Ech hydrogenase. In contrast, the addition of a sodium ionophore did not change the ATP formation rate. These results led to the conclusion that Ech hydrogenase acts as primary proton pump during the oxidation of Fd_{red}.

Under standard conditions, the Fd_{red}-dependent H_2 formation has a $\Delta G^{0\prime}$ value change of -19.3 kJ/mol with midpoint potentials of $Fd/Fd_{red} = -500$ mV and $H_2/2H^+ = -414$ mV. Taking into account the electrochemical ion potential of *Ms. mazei* of -0.18 V the Ech hydrogenase could translocate about one proton per hydrogen molecule formed under standard conditions [35,95]. The analysis of deletion mutants showed that Ech hydrogenase is indeed an important enzyme in aceticlastic methanogenesis of *Ms. barkeri* [92] and *Ms. mazei* [94] because a deletion of the *ech* genes led to an inability of both strains to grow on acetate. Trimethylamine and methanol could still be used as carbon and energy sources by the *Ms. mazei* Δech mutant, but growth rates were lower, less biomass was produced and accelerated substrate consumption was observed [94].

In summary, the Ech hydrogenase acts as primary proton pump and represents an additional energy-coupling site in aceticlastic and methylotrophic methanogenesis when Fd_{red} is formed from acetyl-CoA and formyl-MFR, respectively. Taking these data together, a new model of the Fd: heterodisulfide oxidoreductase system in *Ms. mazei* can be drawn and the long discussed hypothesis of proton translocation by Ech hydrogenase can be confirmed. The current model indicates that H_2 is formed from Fd_{red} as catalyzed by the Ech hydrogenase thereby translocating one proton across the cytoplasmic membrane. The hydrogen molecule diffuses out of the cell and is oxidized by the Mph-reducing hydrogenase (Vho) that transfers electrons to Mph and releases two protons to the extracellular side of the membrane. The last part of the Fd: heterodisulfide oxidoreductase system is the heterodisulfide reductase as terminal enzyme of the anaerobic respiratory chain that also contributes to the electrochemical proton gradient by the transfer of $2H^+/2e^-$ (Figs. 3, 4). Under autotrophic growth conditions, the Ech hydrogenase functions in the reverse direction as compared to respiration (Fig. 3A): it reduces Fd by oxidizing hydrogen to supply low-potential reducing power for CO_2 reduction [90–92]. Additionally, Fd_{red} is needed in biosynthetic reactions to produce acetyl-CoA [100] and pyruvate [101]. However, the reduction of Fd ($E^{0\prime} = -500$ mV [34]) by molecular hydrogen ($E^{0\prime} = -414$ mV) is unfavourable under standard conditions and is highly endergonic in natural habitats with very low partial H_2 pressures (e.g. at a H_2 pressure of 5 Pa $\Delta E\prime = -286$ mV [92]). This is why it has been proposed that the process is coupled to the dissipation of an ion gradient [92,102,103]. Indeed, the reverse reaction of Ech hydrogenase produces Fd_{red} from H_2 coupled to the inflow of protons into the cytoplasm that drives this endergonic reaction.

In *Ms. acetivorans* and probably in *Ms. thermophila*, an active Ech hydrogenase is absent [24,104–106] and its function in Fd-dependent respiration is taken over by the Rnf complex (Fig. 4B) [96,97,105]. Genes encoding the Rnf complex are upregulated under aceticlastic growth conditions [107] and also proteome studies indicate that the Rnf complex is more abundant when acetate is the growth substrate [105]. Furthermore, *Ms. acetivorans* mutants lacking the Rnf complex are unable to grow on acetate [96,97]. Taken these observations together, an important role of the Rnf complex in aceticlastic methanogenesis was assumed. Evidence for this hypothesis comes from the investigation of bacterial Rnf complexes that couple the oxidation of Fd_{red} with the reduction of NAD^+ thereby translocating sodium ions [108,109].
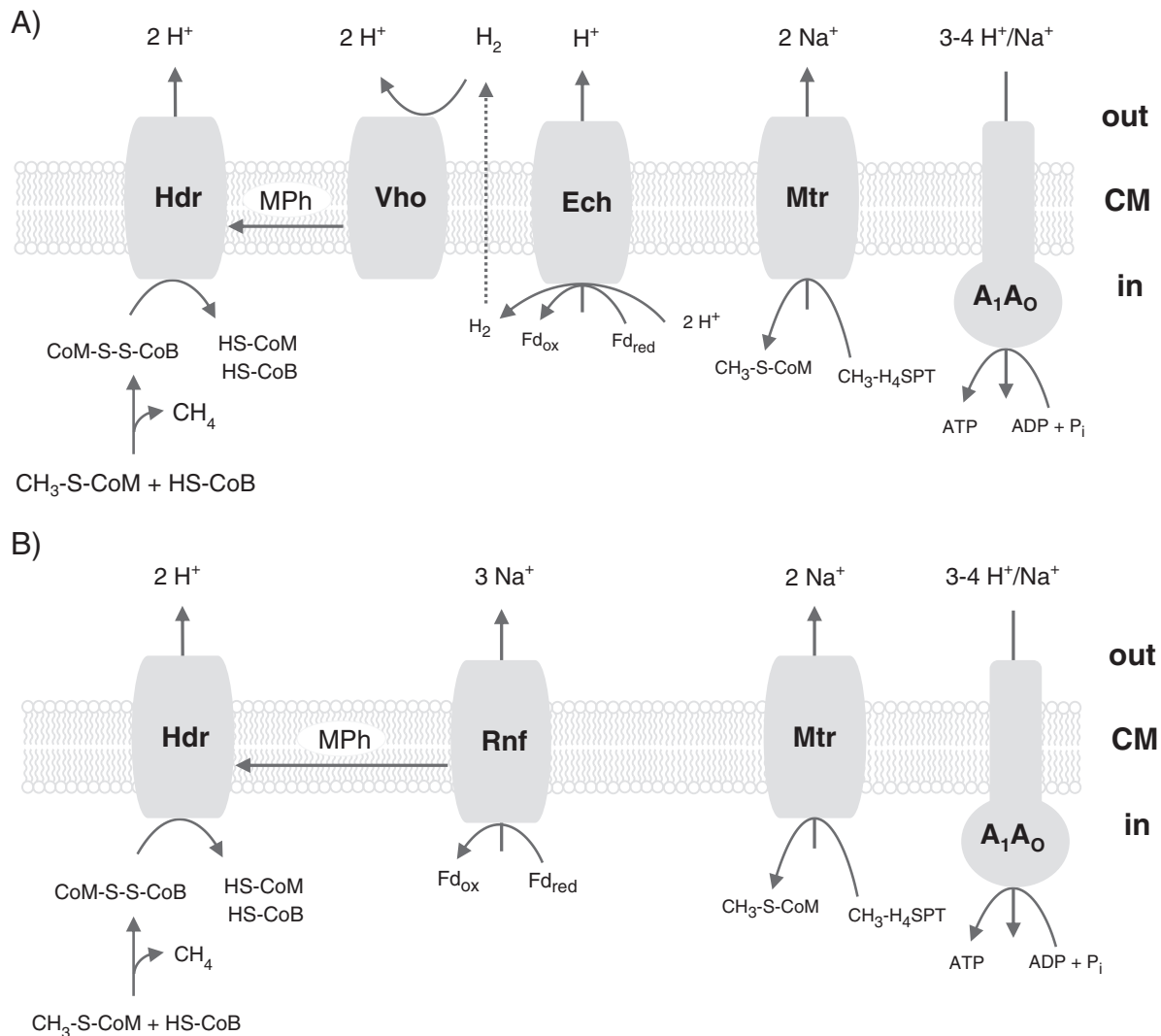
Fig. 4. Process of ion translocation during acetate utilization. (A) *Ms. mazei*, (B) *Ms. acetivorans*. The scheme gives an overview of ion translocation events and does not indicate the mechanism of ion translocation. Vho, Mph-reducing hydrogenase; Ech, Ech hydrogenase; Rnf, Rnf complex; Hdr, heterodisulfide reductase; Mtr, methyl-H_4SPT–coenzyme M methyltransferase; A_1A_O, ATP synthase; CM, cytoplasmic membrane.

Very recently it was demonstrated that the Rnf complex is indeed part of the electron transport chain in *Ms. acetivorans* (Fig. 4B) [96,97]. Furthermore, it was shown that the complex catalyzes Na^+ transport across the membrane coupled to electron transport from Fd_{red} to Mph by a combined approach with ΔRnf mutants and $^{22}Na^+$ transport studies [97]. The overall free energy change of this reaction is −68 kJ/mol that would allow for the translocation of 3 Na^+ per 2 electrons. Thus, this novel coupling site for the electron transport chain not only provides the missing link in the electron transport chain of Ech hydrogenase-negative *Methanosarcina* species but is also the major contributor to the overall energetics of methanogenesis from acetate in *Ms. acetivorans*.

Interestingly, Fd-dependent electron transport in the membrane fractions of the *Ms. acetivorans* ΔRnf and also the *Ms. mazei* ΔEch mutants was still observable [94,97] although the mutant strains were not able to grow on acetate [96,97]. The remaining Fd: heterodisulfide oxidoreductase activity was obviously insufficient to sustain growth on acetate. However, this indicates that in *Ms. acetivorans* and *Ms. mazei* a second membrane protein exists that is able to funnel electrons from Fd_{red} into the respiratory chain. In analogy to *Mt. thermophila*, this role might be fulfilled by the $F_{420}H_2$ dehydrogenase lacking FpoF (Section 6).

5. Characteristics of the key enzymes

In the next chapters the key features of the enzymes involved in membrane bound electron transport of *Methanosarcina* and *Methanosaeta* species will be described.

5.1. Hydrogenases

Five types of hydrogenases have been described in methanogenic archaea, four of which belong to the superfamily of nickel-iron hydrogenases [8,110]. Among the aceticlastic methanogens, H_2 is used as an electron donor by *Methanosarcina* species with the exception of *Ms. acetivorans* that does not produce detectable levels of hydrogenase [106]. *Methanosaeta* strains, in contrast, do not contain annotated hydrogenase genes in their genomes [30–33]. In *Methanosarcina* species that are able to use H_2 as electron donor the F_{420}-reducing hydrogenase (Frh), the Mph-reducing hydrogenase (Vho) and the energy-converting hydrogenase (Ech) are present (Fig. 5). The core of these enzymes is built of a small electron transfer subunit and a large catalytic subunit. The latter subunit contains a binuclear nickel iron centre that is ligated by cysteine residues at the N-terminus (RxCGxCxxxH) and C-terminus (DPCxxCxxH/R) [8]. A gas channel connects the surface with the active
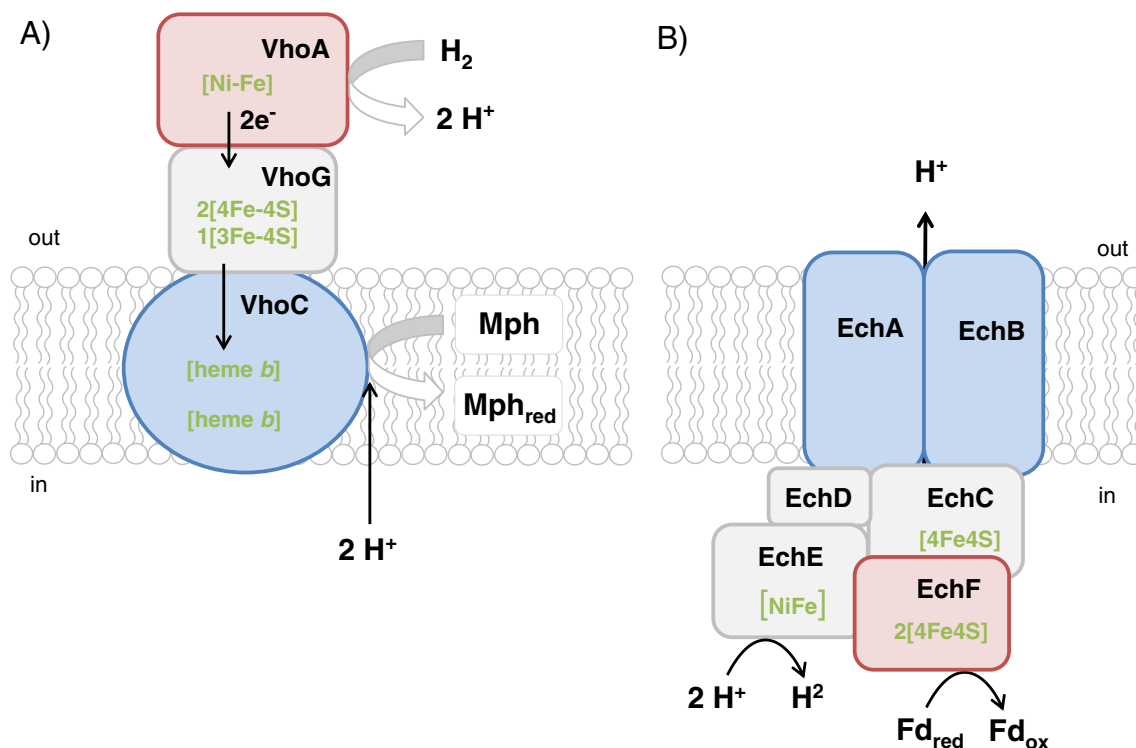
Fig. 5. Structure of hydrogenases. Schematic overview of subunits and prosthetic groups found in the Mph-reducing hydrogenase Vho (A) and Ech hydrogenase (B). Red colour indicates the initial oxidizing subunit, blue colour indicates membrane integral subunits.

site [111]. The small subunit contains three linearly arranged iron–sulfur clusters, a proximal and a distal [4Fe4S] cluster and one central [3Fe4S] cluster [112]. It is responsible for electron transport from the catalytic centre to the surface of the complex [113]. Besides the core subunits methanogenic [NiFe] hydrogenases are equipped with several other polypeptides depending on their physiological function.

In this context, the F_{420}-reducing hydrogenase has to be mentioned. This protein is found in the cytoplasm and is not directly involved in energy conservation in *Methanosarcina* species [87,114]. The enzyme is involved in hydrogenotrophic methanogenesis and provides $F_{420}H_2$ for the reduction of methenyl-H4SPT to methyl-H4SPT. In addition to the small and large subunit the complex contains an FAD carrying subunit (FrhB) that is able to reduce F_{420} [8] and is homologous to FpoF (Section 5.3).

5.1.1. Methanophenazine-reducing hydrogenase

This type of hydrogenase is only found in methanogens that contain cytochromes such as *Methanosarcina* species and other members of the family Methanosarcinaceae (Fig. 5A). The protein is membrane bound and can be purified only in the presence of detergents [115,116]. The structural genes of the Mph-reducing hydrogenase are arranged in the order *vho*G–*vho*A that were identified as those encoding the small and the large subunit of the NiFe hydrogenase from *Ms. mazei* [117]. An additional open reading frame (*vho*C) encodes a membrane spanning cytochrome *b* [118–120]. Later on it was found that in *Ms. mazei* three isoenzymes are present (VhoGAC, VhtGAC, VhxGAC) that are almost identical and cannot be separated by purification [115]. Therefore, the isoenzymes are combined and are referred to as Mph-reducing hydrogenases (Vho) in this review. Comparison of the sequencing data of VhoG with the experimentally determined N-terminus of the small subunit indicates the presence of a Tat-dependent leader peptide, whereas the large subunit lacks any known targeting signal for export. Therefore, it is evident that the large subunit is cotranslocated with the small subunit across the cytoplasmic membrane. Overall, the Mph-reducing hydrogenase is highly homologous to many membrane bound cytochrome *b*

containing hydrogenases from bacteria and it has been shown that at least part of the large subunit of the enzyme from bacteria is exposed towards the periplasm [121]. Therefore, it is highly probable that the active centre of the Mph-reducing hydrogenase is also located at the extracellular face of the membrane. All amino acid residues involved in the ligation of the Ni-Fe centre and of the iron–sulfur clusters are conserved in the small subunit (VhoG) and the large subunit (VhoA) of Mph-reducing hydrogenase in *Ms. mazei*, indicating that the [3Fe4S] cluster and both [4Fe4S] clusters are present.

Electron transport studies with *Ms. mazei* membrane vesicles showed the direct involvement of Mph-reducing hydrogenase in energy conservation [84,120]. The enzyme was able to couple the oxidation of H_2 with the reduction of its cytochrome *b* subunit and finally transferred electrons to the water-soluble Mph analogue 2-OH-phenazine. Overall, the reaction led to proton translocation with a stoichiometry of about $2H^+/2e^-$. Later on it was shown that also the native cofactor serves as electron acceptor of the Mph-reducing hydrogenase [47].

Combining all published results it is possible to speculate about the reaction mechanism of the Mph-reducing hydrogenase (Fig. 5A). The first reaction involves the oxidation of H_2 by the bimetallic NiFe centre of the large subunit. The remaining protons are released into the extracellular space. The three linearly arranged iron–sulfur clusters of the small subunit transfer the electrons to the heme groups present in the membrane-integral cytochrome *b* subunit. In the last step, the cytochrome *b* subunit reduces Mph with the help of two protons from the cytoplasm. Hence, the overall process leads to the formation of two scalar protons.

5.1.2. Ech hydrogenase

In *Ms. mazei* and *Ms. barkeri*, Ech hydrogenase (*energy-conserving hydrogenase*) [102] (Fig. 5B) is responsible for membrane bound Fd_{red} oxidation (Section 4.3). The protein belongs to the phylogenetically distinct group of multisubunit [NiFe] hydrogenases [122] that couple hydrogen formation in the course of (poly)Fd oxidation with ion translocation. Hydrogenases of the Ech-type are thought to be among the

most ancient energy-conserving proteins [110,123] and various microorganisms were shown to contain Ech-type hydrogenases. Some examples are the Coo [NiFe] hydrogenases of *Rhodospirillum rubrum* [124] and *Carboxydothermus hydrogenoformans* [125], the Hyc and Hyf [NiFe] hydrogenases of *Escherichia coli* [126,127] (also termed *E. coli* hydrogenases 3 and 4, respectively) and the Mbh hydrogenase of *Pyrococcus furiosus* that was demonstrated to translocate protons in the process of Fd_{red} oxidation [128].

Ech hydrogenases from *Ms. mazei* and *Ms. barkeri* contain six protein subunits encoded in one operon (*echABCDEF*) that is highly upregulated under aceticlastic growth conditions [129]. The enzyme consists of the classical small and large hydrogenase subunits (EchC and EchE) of [NiFe] hydrogenases with the large subunit harbouring four conserved cysteine residues to coordinate the binuclear [NiFe] active site (Fig. 5B). EchC contains one of the three [4Fe4S] clusters; the other two are coordinated by the hydrophilic subunit EchF [93]. The three clusters give rise to $S_{1/2}$ electron paramagnetic resonance (EPR) signals of $g = 1.96$, $g = 1.89$ and $g = 1.92$ [130] with the latter two exhibiting a pH-dependent shift in their redox potential. Forzi et al. [131] propose that electrons deriving from the $H_2 \rightarrow 2H^+ + 2\,e^-$ reaction at the [NiFe] centre migrate to the proximal [4Fe4S] cluster in EchC towards the two clusters in EchF to be finally released from Ech hydrogenase to reduce a 2[4Fe4S] Fd [93,131]. The Ech hydrogenase contains another hydrophilic subunit (EchD) and two additional hydrophobic, membrane bound subunits (EchA and EchB, [93,132]). The isolated Ech hydrogenase of *Ms. barkeri* reduced and oxidized a 2[4Fe4S] Fd purified from the same organism with high specificity (K_m values of 1 and 7.5 μM for the reductive and oxidative reaction, respectively) and concomitant oxidation or reduction of H_2 and H^+, respectively [92,93]. These results indicated that Ech hydrogenase forms the link between the CO dehydrogenase/acetyl-CoA synthase reaction [55,100] and membrane bound electron transport [92,93] by oxidizing Fd_{red} that derives from the oxidation of acetyl-CoA. The Ech hydrogenase does not interact directly with Mph [93,94] but is dependent on the action of the Mph-reducing hydrogenase (Sections 4.3 and 5.1.1) to funnel electrons into the Mph pool. Regarding the ion translocating properties, it has long been suggested that Ech hydrogenase is a site of ion translocation in methanogenic bioenergetics [102,103,133]. Even before Ech hydrogenase was recognized, experiments with resting cell suspensions indicated that the steps involving Ech hydrogenase were linked to energy conservation and ion translocation [98,134] which was further substantiated by mutational studies of *Ms. barkeri* lacking Ech hydrogenase [92,135]. In 2010, we unequivocally demonstrated that Ech hydrogenase translocates protons coupled to Fd_{red} oxidation and hydrogen evolution in *Ms. mazei* [95] identifying this enzyme as additional site of energy conservation in methanogenic bioenergetics. Regarding the mechanism of proton translocation in Ech hydrogenase it is useful to study the similarities [136] and common ancestry [102,110,133,136–139] of Ech hydrogenase and NADH dehydrogenase I. This is particularly useful because a crystal structure of NADH dehydrogenase I (complex I) exists [140–142] that may give an insight into the proton translocation machinery of Ech hydrogenase. One of the key components in a redox-driven proton pump is the coupling of the electron transport to the conformational change of the protein complex allowing the translocation of protons. Although the structure of Ech hydrogenase is not known, homology modelling to complex I [136] suggests that the coupling site of Ech hydrogenase is formed at the interface of the subunits EchC, EchE and EchB. The cavity between EchC and EchE (small and large hydrogenase subunits) forms the interaction site between the hydrophilic subunits and the hydrophobic membrane-spanning arm (EchAB) with EchB as a membrane-integral interaction partner to EchCE. Interestingly, the small and large hydrogenase subunits of Ech-type hydrogenases are more closely related to NADH dehydrogenase I than to the corresponding subunits of soluble [NiFe] hydrogenases [143]. In the much larger NADH dehydrogenase, part of the conformational change is originating from the reduction of cluster

N2 (homologous to the proximal [4Fe4S] cluster in EchC) leading to a disconnection of cysteine residues and a subsequent conformational change [144]. However, in [NiFe] hydrogenases, these cysteines are absent [136] and structural analyses of soluble [NiFe] hydrogenases indeed show that there is no conformational change upon reduction of the cluster [145].

Another part of conformational change in NADH dehydrogenase probably originates from the quinone reduction reaction that releases the majority of the redox energy [145]. Due to the similarity of the hydrogenase reaction ($2H^+ + 2\,e^- \rightarrow H_2$) to the quinone reduction reaction ($Q + 2H^+ + 2\,e^- \rightarrow QH_2$) as well as the high conservation of EchB cytoplasmic loops, Efremov and Sazanov [136] assume that the hydrogenase reaction leads to a conformational change in Ech hydrogenase mediated by EchB towards EchA. EchA is homologous to the *Bacillus subtilis* Na^+/H^+ antiporter subunit MrpA [133,137,146] and is probably responsible for the translocation of the proton.

5.2. The Rnf complex

The first Rnf-type complex was discovered in the bacterium *Rhodobacter (R.) capsulatus* [147] where it was shown that a deletion of the *rnf* genes leads to a loss in nitrogen fixation. Later on it was demonstrated that the Rnf complex has a Fd: NADH oxidoreductase function in *Acetobacterium (A.) woodii* [108,109,148–150] and *Clostridium ljungdahlii* [151] and presumably many other bacteria [152–156]. It shows similarities to the sodium translocating NADH quinone oxidoreductase complex of bacteria that has a different evolutionary ancestry than complex I [157,158].

The Fd: Mph oxidoreductase system of *Ms. acetivorans* is formed in part by the membrane bound Rnf complex (Fig. 4B) [96,97]. The gene cluster containing the classical *rnf* genes *rnfABCDGE* is co-transcribed with two additional genes at the beginning and the end of the operon, respectively [105]. The gene at the beginning of the *rnf* gene cluster encodes a multi-heme cytochrome that was shown to be part of the Rnf complex in *Ms. acetivorans* [96]. The additional gene at the end of the gene cluster encodes a small hydrophobic protein that has no homology to genes with a known function [105].

As the *Ms. acetivorans* Rnf complex (Fig. 6) has not yet been purified, the here presented analysis of the Rnf subunits has mostly been performed by sequence analysis and comparison to the better investigated bacterial Rnf complexes of *R. capsulatus* and *A. woodii*. The Rnf complex of *Ms. acetivorans* seems to be firmly integrated into the cytoplasmic membrane by the subunits RnfA, RnfD and RnfE. RnfA and RnfE of the *E. coli* Rnf complex were shown to be tightly membrane bound [159] and are not predicted to contain any cofactors. Whereas the C- and N-termini of the *E. coli* RnfA are directed towards the periplasm, the RnfE C- and N-termini face the cytoplasmic site. Saaf et al. [159] state that the RnfA/E subunits form a quasi-symmetrical complex possibly involved in electron transfer or channel formation. Besides being bound to the membrane, the *Vibrio (V.) cholerae* RnfD subunit was demonstrated to contain a FMN cofactor covalently bound to Thr-187 that is located at the periplasmic side of the protein [160]. This threonine is a conserved residue and the corresponding FMN binding site is present in a variety of RnfD subunits of other bacteria [155,160]. This residue is not conserved in the *Ms. acetivorans* RnfD subunit and the FMN prosthetic group is probably missing. As the function of the FMN cofactor is unknown, it is not possible to speculate about the biological implications for the *Ms. acetivorans* Rnf complex. RnfG is membrane-associated and probably bound to the membrane with one transmembrane helix as inferred from homology with the *A. woodii* RnfG [149,155]. The *V. cholerae* RnfG contains an FMN covalently bound to Thr-175 [160] that is conserved in *A. woodii* (Thr-185, [149]) and also in *Ms. acetivorans* (Thr-166). In *V. cholerae* and *A. woodii*, it is located at the periplasmic side of the membrane indicating that also in *Ms. acetivorans* an FMN cofactor could face the extracellular space. Although the crystal structure of an RnfG homologue from *Thermotoga maritima* was solved
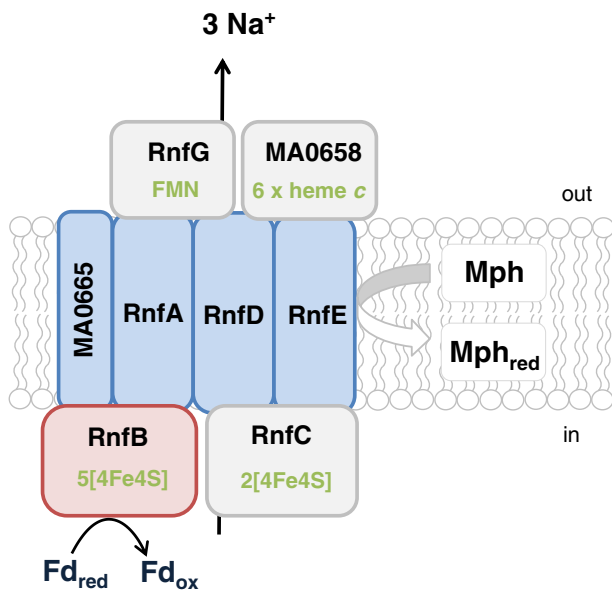
Fig. 6. Rnf complex. Tentative model of the Rnf complex of *Ms. acetivorans*. The additional small hydrophobic subunit (MA0665) is indicated as part of the membrane module. The multi-heme cytochrome *c* is termed MA0658. The exact topology of the subunits, the electron flow and the sodium ion translocation mechanism have not been determined in the methanogenic enzyme. Red colour indicates the initial oxidizing subunit, blue colour indicates membrane integral subunits.

(Protein Data Bank (PDB) ID: 3DCZ, Joint Center for Structural Genomics (JCSG)), the function of this FMN cofactor is not known. RnfB is probably membrane-associated with one to three transmembrane helices. More interestingly, it contains conserved cysteine residues that might coordinate iron–sulfur clusters [105]. Starting at positions Cys-172, Cys-227 and Cys-246, three classical C–$(X)_2$–C–$(X)_2$–C–$(X)_3$–CP motifs are present that might coordinate three [4Fe4S] clusters. Bioinformatical analysis indicates that an additional cluster might be coordinated by a cysteine-rich motif starting at Cys-138 with the sequence C–$(X)_3$–C–$(X)_5$–C–$(X)_3$–CP [161]. In addition, a fifth iron–sulfur cluster might be coordinated by an N-terminal domain with the consensus sequence C–$(X)_2$–C–$(X)_4$–C–$(X)_{16}$–CP starting at Cys-50 in the *Ms. acetivorans* RnfB subunit. However, the cofactor content of RnfB remains to be elucidated experimentally. RnfC is a subunit that is tightly associated with the membrane although it is not membrane bound [149,157]. The C–terminus contains two conserved C–$(X)_2$–C–$(X)_2$–C–$(X)_3$–CP motifs indicating the binding of two [4Fe4S] clusters [147,162]. It was suggested that the RnfC subunit binds FMN [157,163,164] but this has so far not been demonstrated experimentally. Furthermore, RnfC is thought to be the NADH-interacting subunit [157]. The *R. capsulatus* RnfC contains a conserved region [157] highly homologous to bacterial NAD$^+$-reducing hydrogenases [165–167], bacterial complex I [163,164] and mitochondrial complex I [168,169]. However, this region (residues 122–155) is hardly conserved in RnfC of *Ms. acetivorans* and experimental results validate that the methanogenic complex does not interact with NADH/NAD$^+$ [96,97]. The *Ms. acetivorans* Rnf complex also contains a *c*-type cytochrome subunit [105]. It is membrane bound and represents so far the only *c*-type cytochrome with an assigned function in methanogens [96], namely the electron transport from the Rnf complex to methanophenazine. Sequence analysis identifies five CXXCH and one CXXXCH motifs that could bind six heme *c* groups. The membrane fraction of *Ms. acetivorans* exhibits a peak at 554 nm upon reduction with Fd$_{red}$ so the cytochrome can be characterized as a c_{554}-cytochrome [96].

The *Ms. acetivorans* Rnf complex oxidizes Fd$_{red}$, presumably with the polyferredoxin-like subunit RnfB [155]. How electrons finally reach the multi-heme *c*-type cytochrome subunit to reduce Mph is not known but probably involves the iron–sulfur clusters of RnfC and the FMN cofactor

of RnfG. Biegel et al. [155] suggest that the membrane bound subunits RnfA, RnfD and RnfE are responsible for the Na$^+$ translocation of the *A. woodii* Rnf complex. However, the exact mechanism of electron transport and ion translocation remains to be elucidated.

5.3. Characteristics of the F$_{420}$H$_2$ dehydrogenase

The F$_{420}$H$_2$ dehydrogenase (also named Fpo = F$_{420}$:phenazine oxidoreductase) is found only in members of the order Methanosarcinales and is absent in obligate hydrogenotrophic methanogens (Fig. 7). From the point of view of the authors it is one of the most fascinating enzymes found in methanogenic archaea. As described in Section 4.2, the protein uses F$_{420}$H$_2$ as electron donor and reduces the quinone analogue methanophenazine [46]. Analysis of the proton-translocating activity of the F$_{420}$H$_2$ dehydrogenase showed that the enzyme can transfer two protons across the membrane in the course of the reaction cycle. This finding is in agreement with thermodynamic considerations as indicated in Section 4.2. Hence, it represents an intrinsic proton-translocating complex in members of the order Methanosarcinales that significantly contributes to the formation of the $\Delta\mu_{H+}$.

When the genome of *Ms. mazei* was sequenced it became evident that the enzyme is encoded by 14 genes (*fpoABCDFHIJ1J2KLMNO*) [23] that form an operon structure. The gene encoding the electron input subunit FpoF has a different chromosomal location than the other *fpo* genes. Hydropathy plots revealed that the deduced subunits from Fpo A, H, J, K, L, M and N are membrane-integral components forming more than 50 transmembrane helices. A 115 kDa subcomplex of the holoenzyme was purified comprising the hydrophilic subunits FpoBCDI and FpoF. The latter subunit contained one flavin and two iron–sulfur (FeS) clusters [170]. The other subunits contained three FeS clusters. Later on a F$_{420}$H$_2$ dehydrogenase complex with a size of 400 kDa could be partially purified that was capable of F$_{420}$H$_2$ oxidation and phenazine reduction, indicating the structural integrity of the complex (unpublished results). However, up to now it was not possible to purify the holoenzyme to homogeneity.

The amino acid sequences deduced from the genome sequence of *Methanosarcina* species showed that the F$_{420}$H$_2$ dehydrogenase is highly homologous to bacterial and eukaryotic proton-translocating NADH: quinone oxidoreductases (complex I). During the last years attempts to crystallize bacterial complex I were successful and the three-dimensional structure has recently been described by Sazanov and co-workers. The results comprised the elucidation of the eight-subunit hydrophilic domain of the *Thermus (T.) thermophilus* complex I up to 3.1 Å resolution [144,171] and the analysis of the entire *T. thermophilus* complex I at 4.5 Å resolution [140]. Subsequently, the crystal structure of the membrane domain from the *E. coli* complex I (missing Nqo8/NuoH) with a resolution of 3.0 Å was described [141]. Finally, the structure of the isolated *T. thermophilus* membrane domain containing subunit Nqo8 was also solved [142] leading to the elucidation of the entire structure of complex I from *T. thermophilus* at 3.3 Å resolution [142].

The high homology of the F$_{420}$H$_2$ dehydrogenase to complex I of *T. thermophilus* prompted us to speculate about the structure and function of the subunits in the methanogenic protein. For this purpose the amino acid sequences of the F$_{420}$H$_2$ dehydrogenase (with exception of FpoF and FpoO that are not present in complex I) were analysed by the protein structure prediction servers Cn3D 4.3 and RaptorX [172,173] using the 3D structures of the subunits of complex I from *T. thermophilus* as scaffold (PDB ID: 4HEA). Almost all the amino acid sequences of the Fpo subunits could be modelled into the given structure of complex I (not shown) with the exception of subunit FpoJ1 and FpoJ2 of the methanogenic enzyme. Small differences in models between subunits of Fpo and Nqo were due to short insertion of amino acid stretches (3–11 AS) and differences in the length of the N- and C- termini. Based on the modelling it is tempting to speculate on the catalytic mechanism of the Fpo complex and the critical structural elements involved in electron transfer and H$^+$ translocation.
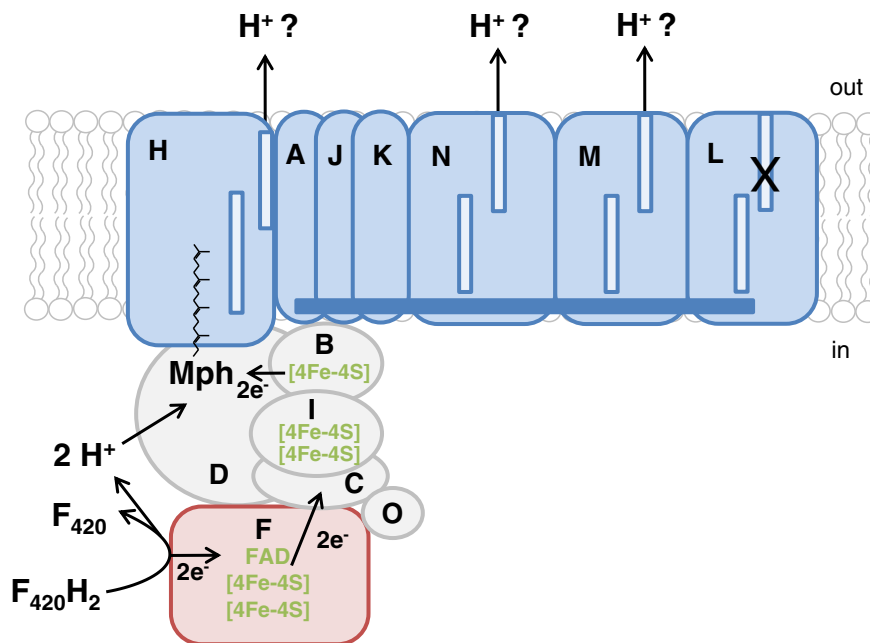
Fig. 7. Tentative model of the $F_{420}H_2$ dehydrogenase. The figure indicates the subunit arrangement, prosthetic groups and the electron flow. Predicted discontinuous TM helices in FpoHLMN are shown as light blue boxes. Putative helix HL is indicated by a dark blue box. Question marks indicate that the exact site of H^+ translocation is not known. The predicted discontinuous TM helix of FpoL is marked by X because it might be inactive. The function of the hydrophilic subunit FpoO is not known. Therefore, its properties are not discussed. Red colour indicates the initial oxidizing subunit, blue colour indicates membrane integral subunits.

a) In complex I of *T. thermophilus* subunits Nqo1, 2, and 3 serve as module for electron input from NADH into a chain of FeS clusters found in Nqo9 and Nqo6 [144,171]. Homologues of the genes encoding Nqo1, 2, and 3 are absent from the genome of *Methanosarcina* species. Instead, it was shown that subunit FpoF functions as an electron-feeding device for the $F_{420}H_2$ dehydrogenase.

FpoF is an iron–sulfur flavoprotein that contains one FAD and two [4Fe4S] clusters per single protein subunit (Fig. 7) [86]. The FpoF protein is not homologous to the Nqo 1, 2, and 3 proteins, which is on the one hand not surprising because it oxidizes $F_{420}H_2$ and not NADH. On the other hand, the functional similarity as electron input module leads to a similarity in cofactor content: both proteins contain a flavin to enable the switch from the two electron donors NADH/$F_{420}H_2$ to the one-electron accepting FeS clusters that are also present in both subunits. FpoF is homologous to the FrhB subunit of the F_{420}-reducing hydrogenase (FrhABG) [174]. Recently, the structure of the FrhABG complex was modelled into data obtained by cryo-electron microscopy [175]. After refinement, a resolution of about 4 Å for the FrhABG complex was reached. The modelling revealed that the FpoF homologue FrhB contains a novel fold not previously reported [175]. On the surface of the protein, a distinctive ~35 Å surface helix was observed that corresponds to the C-terminal helix. The core of the protein is formed by a mixed six-stranded beta sheet. Modelling of electron densities of cryo-electron microscopy data with and without F_{420} revealed that the cofactor is probably located at a distance of 4 Å to the flavin isoalloxazine ring inside a large pocket surrounded by conserved residues [175]. Part of the F_{420} binding site is built by the FrhB residues S209 and V210 that are located in a loop between two beta strands. In FpoF, this corresponds to the conserved S272 and V273 residues. These residues are part of a conserved sequence motif that is presumably used for F_{420} binding. The consensus motif in FrhB homologues is GXhG (h, hydrophobic residue), the actual sequence motif in FpoF is GSVG. Another conserved region that is part of a three-stranded beta sheet flanked by two short helices and probably involved in F_{420} binding, is the conserved 163IGKGK region in FrhB. In FpoF, this region is 225FTKGK. The consensus sequence as compared to other FrhB homologues is [LIFYHW]-X-[RK]-G-[RK]. It forms a turn

that is situated close to the position of the isoalloxazine ring of F_{420} [175] and might enable one or two of the conserved lysine residues to interact with the phosphate group of F_{420}. Besides the interaction with $F_{420}H_2$ when FpoF is bound to the Fpo complex, purified FpoF can also interact with Fd and oxidizes Fd_{red} with high specificity (K_m for Fd = 0.5 μM) [86].

b) The membrane associated module of complex I is constituted of Nqo4, 5, 6 and 9 [171] that connects the NADH-oxidizing unit to the membrane-integral subcomplex. The corresponding counterparts in the $F_{420}H_2$ dehydrogenase are FpoB, C, D and I (Fig. 7). In complex I, electrons are channelled from the input module (containing flavin and different FeS clusters as described above) via the FeS groups N6a and N6b to the terminal cluster N2, located in close vicinity to the quinone-binding site [171]. Subunit Nqo9 coordinates the tetranuclear clusters N6a and N6b that are similar to the 2 [4Fe4S] Fd family. Clusters N6a and N6b are coordinated by cysteines 53, 56, 59, and 108, and by cysteines 63, 98, 101, and 104, respectively. Cluster N2 is found in subunit Nqo6 and is bound by C45, C46, C140 and C111. The unique coordination of cluster N2 by two consecutive cysteines is obviously important for the electron transfer to quinone that is bound at the interface of the hydrophilic subunits and the membrane domain (see below) [142]. Sequence homology and model comparison indicated that identical binding motifs for [4Fe4S] clusters are present in FpoI and FpoB. Hence, it is tempting to speculate that the FeS clusters are coordinated by C44, C47, C50, C94 and C54, C84, C87, C90 in the case of FpoI and C61, C62, C156, C126 in the case of FpoB, which includes the tandem cysteine motif. In summary, it is highly probable that electron transport in the membrane associated module of the Nqo complex and the $F_{420}H_2$ dehydrogenase is very similar. Besides the electron transfer function, the membrane-associated module of Nqo is also responsible for quinone reduction, which will be described in the next section.

c) Quinone reaction chamber

Before the structure was elucidated, experimental evidence had already been found that the C-terminal end of Nqo4 is the binding site of the polar head of quinones, whereas the hydrophobic tail of the electron acceptor is bound to the membrane-integral subunit

Nqo8 [176]. The structural analysis revealed that the quinone binding site in complex I of *T. thermophilus* [142] forms a long and narrow cavity and the reactive head of the quinone is in effective electron transfer distance of the FeS cluster N2. Important structures for the formation of the quinone chamber are TM1, TM6 and amphipathic AH1 of Nqo8 and of TM1 from Nqo7 as well as hydrophobic areas of subunits Nqo4/6. The residues lining the chamber of Nqo8 and Nqo6 [142] are all highly conserved in FpoH and FpoB, respectively. However, some residues in FpoB (G63, V64, and I67) possess smaller side chains compared to their counterpart in Nqo8 (A47, I48 and M51). In contrast, the residues in Nqo4 that form part of the hydrophilic quinone-binding site are not conserved in FpoD. This finding is not surprising, because the electron acceptor of the $F_{420}H_2$ dehydrogenase, Mph, is structurally different from quinones. Especially the phenazine ring system is much larger and probably needs more space in comparison to the quinone ring. In contrast, the hydrophobic part of Mph made up of 5 isoprenoid units is structurally similar to the tail of quinones and might fit into a hydrophobic cavity that is similar to the one in the Nqo complex.

d) Connection between the Q-site and membrane subunits: the E-channel

Most of the interactions between the hydrophilic and the membrane bound part of the Nqo complex involve subunit Nqo8 [142]. Most striking is the fact that Nqo8 and Nqo10/11 form antiporter-like half channels that are connected by the Nqo8 residues E130, E163, E213 and Nqo7-D72 (referred to as E-channel). Thus, redox reactions in the Q-site lead to conformational changes in the half channels. These are caused by a chain of charged or polar residues that start from the Q-binding site and reach deep into the membrane. As a result of conformational changes in the E-channel it is likely that this chain of charged residues drive the transport of protons across the membrane [142]. The comparison of subunits Nqo6, 7, 8, 10, and 11 showed that almost all of the residues forming the E-channel are found in the corresponding positions in the homologous subunits FpoB, A H, J and K indicating that the E-channel might also be structural element of the $F_{420}H_2$ dehydrogenase.

e) Function of the antiporter-like subunits Nqo12–14

The membrane integral subunits Nqo12–14 reach from Nqo8 to the far end of the L-shaped complex [140–142]. These subunits share a structurally similar core of 14 TM helices. Among them are discontinuous TM helices (TM7 and 12) that are likely to be involved in H^+ translocation. In addition to the core helices, Nqo12 contains the long amphipathic transversal helix HL that directly interacts with the discontinuous TM helices of Nqo12–14 by a piston-like motion. It probably represents the coupling element between redox reaction and H^+ translocation. The molecular piston is driven by redox changes in cluster N2 and the quinone-binding site leading to conformational changes in subunits Nqo7, 8,10, and 11 that are

directly connected to the HL helix of Nqo12. The movement of HL drives a conformational change in the discontinuous helices of Nqo12–14 leading to the translocation of three protons. Together with the transfer of one H^+ through the E-channel the experimentally determined ratio of $4H^+/2e^-$ can be explained in a very convincing way. The counterparts of Nqo12–14, subunits FpoLMN of the $F_{420}H_2$ dehydrogenase align very well with the core helices of Nqo12–14 and also the transversal helix HL was detected in FpoL. In addition, essential charged residues found in the Nqo12–14 discontinuous helices [141,177] are highly conserved indicating that the discontinuous TM helices (TM7 and 12) could be present in FpoLMN.

In summary, the overall structure of the critical elements for proton translocation is obviously conserved between complex I and $F_{420}H_2$ dehydrogenase. However, alignments and modelling indicated that FpoL contains an insertion of 6 amino acids in discontinuous helices TM12 (position 414–419) (Fig. 8) that could lead to structural modification and a loss of function (Fig. 7). The finding that the coupling efficiency of $F_{420}H_2$ dehydrogenase is only half of the one of complex I ($2H^+/2e^-$) is in line with this assumption. Besides the alterations in FpoL another coupling site in the $F_{420}H_2$ dehydrogenase might not be functional or shut down, leaving two coupling sites. This hypothesis is supported by the fact that the midpoint potential of Mph/Mph$_{red}$ is in the range of -165 mV. Combined with the oxidation of $F_{420}H_2$ (-360 mV) the $\Delta G^{0\prime}$ value is only -37.6 kJ/mol compared to a $\Delta G^{0\prime}$ of -80.9 kJ/mol for the NADH-dependent reduction of ubiquinone. In this connection, we also refer to Section 6 where the system of energy conservation in *Methanosaeta* species is discussed.

However, there are remarkable similarities between complex I and the $F_{420}H_2$ dehydrogenase, indicating that the methanogenic enzyme belongs to the family of enzymes that couple the oxidation of soluble electron donors and reduction of membrane integral quinones and quinone analogues with the translocation of ions against the membrane potential. Our brief comparison of $F_{420}H_2$ dehydrogenase and the Nqo complex omitted most of the marvellous details on structure and reaction in the bacterial enzyme. Further studies using more sophisticated protein modelling programmes are needed to confirm the observed differences with respect to the input module and the binding of Mph and to solve the problem of the mechanisms of energetic coupling in the $F_{420}H_2$ dehydrogenase that could be based on the shutdown of one or two of the four proton channels found in complex I.

5.4. Characteristics of the heterodisulfide reductase

In methanogenic archaea, two different types of heterodisulfide reductases exist. The soluble heterotrimeric HdrABC enzyme performs electron bifurcation [68] via the flavin-containing subunit HdrA

Fig. 8. Alignment of the discontinuous transmembrane helix 12 in FpoL. Numbering is according to NuoL from *E. coli* (M. Sato et al. [177]). Residues forming TM12 are indicated by a yellow box. Alignment was performed with Clustal Omega (http://www.ebi.ac.uk/Tools/msa/clustalo/). Amino acid sequence identification numbers (from top to bottom): YP_490518, NP_006964, CAB44520, AAA97949, ADB78261, AGS44097, ADE30356, NP_085478, YP_843482, YP_004385204, AAF65739, NP_616438.

[16,68]. Electrons are delivered by the associated hydrogenase Mvh [68], are bifurcated at the flavin in HdrA and are subsequently used to couple the exergonic reduction of the heterodisulfide (catalyzed by HdrBC) to the endergonic reduction of ferredoxin (Section 3.3) [16,34,68]. The second type of heterodisulfide reductase is the membrane bound HdrDE enzyme only present in the cytochrome-containing Methanosarcinales (Fig. 9) [34]. Members of the HdrDE protein family do not perform electron bifurcation and lack a homologue to the flavin-containing subunit HdrA. Instead, HdrDE couples Mph_{red} oxidation to the reduction of the heterodisulfide [84] with concomitant proton extrusion [84,97]. Thus, it serves as the terminal reductase in the anaerobic respiratory chain of cytochrome-containing methanogens.

The HdrDE enzyme is firmly integrated into the membrane by the cytochrome-containing subunit HdrE, which contains two b-type hemes (Fig. 9) [178–180]. In the *Ms. thermophila* enzyme, one heme group is high-spin, hexacoordinated and has a high midpoint potential of -23 mV whereas the second heme group is low-spin, pentacoordinated and has a low midpoint potential of -180 mV [178]. Only the low-spin heme seems to be involved in catalysis [181] whereas the exact function of the high-spin heme remains unknown. The HdrD subunit forms the catalytic centre and contains two characteristic cysteine-rich motifs ($CX_{31-32}CCX_{33-38}CXXC$, [182]) that coordinate two [4Fe4S] iron–sulfur clusters. The apparent midpoint potentials for the two clusters are -100 mV and -400 mV, respectively [178,181]. The low-potential cluster is not involved in redox cycling but instead has a role in the stabilization of a radical intermediate. The absence of a prosthetic group that could donate two electrons at once to the heterodisulfide leads to a step-wise one-electron reduction of the CoM-S-S-CoB creating a coenzyme M thiyl radical intermediate [178,183]. This intermediate requires the low potential [4Fe4S] cluster in order to remain stable and accessible for the second one-electron reduction that leads to the formation of HS-CoM and HS-CoB [182]. Hence, the electron flow within HdrDE probably proceeds as follows: $Mph_{red} \rightarrow heme\ b_L \rightarrow [4Fe4S]_H \rightarrow CoM\text{-}S\text{-}S\text{-}CoB$. Reduction of the heterodisulfide happens at the $[4Fe4S]_H$ cluster, which was extensively studied by different spectroscopic methods. However, the exact binding of the heterodisulfide to the cluster remains to be elucidated. For a detailed discussion of this FeS cluster the reader is kindly referred to the review written by Hedderich et al. [182]. Simianu et al. [178] suggested that the proton translocation mechanism of the heterodisulfide

reductase is similar to the quinone-dependent proton translocation mechanism of the bacterial bc_1 complex. Two protons would directly be released to the extracellular space upon partial oxidation leaving Mph in a state corresponding to the semiquinone state. A subsequent one-electron oxidation step would leave Mph in its fully oxidized state. However, this mechanism has neither been confirmed nor rejected by subsequent studies.

6. Novel aspects on energy conservation in *Methanosaeta thermophila*

The energy conservation pathway of *Methanosaeta* species is less well understood than that of the members of the genus *Methanosarcina*. Part of the reason is that *Methanosaeta* species are less versatile and solely depend on acetate as carbon and energy source. Thus, e.g. mutant generation of central energy metabolism enzymes is not feasible. In addition, there is no genetic manipulation system available to create deletion mutants of *Methanosaeta* species. However, central features of the energy conservation pathway have been investigated recently and will be discussed.

The presence of the acetyl-CoA synthetase in *Methanosaeta* species implies that two ATP equivalents are required for the activation of one molecule of acetate whereas in *Methanosarcina* species only one ATP is used for acetyl-CoA formation (see Section 3.2 for more details and references therein). As a by-product, the acetyl-CoA synthetase forms pyrophosphate that might be used by members of the genus *Methanosaeta* to compensate for the ATP expense in the acetate activation reaction. The most prominent possibility is the hydrolysis of pyrophosphate by an ion-translocating, membrane bound pyrophosphatase. Such enzymes have been characterized in *Ms. mazei* [184,185] but are also present in other methanoarchaea [184]. However, the genomes of *Mt. thermophila*, *Mt. harundinacea* and *Mt. concilii* [30–32] revealed that membrane bound pyrophosphatases are not present in these organisms. The K_m value of the *Mt. thermophila* soluble pyrophosphatase is relatively high (0.3 mM, [28]) which might allow other enzymes to make use of part of the pyrophosphate for the phosphorylation of other cellular compounds. However, the number of described pyrophosphate-using phosphorylating enzymes is very limited. *Mt. thermophila* does not contain genes encoding a pyrophosphate-dependent phosphofructokinase [28,186] whereas one gene shows a low but significant homology to the gene encoding pyruvate phosphate
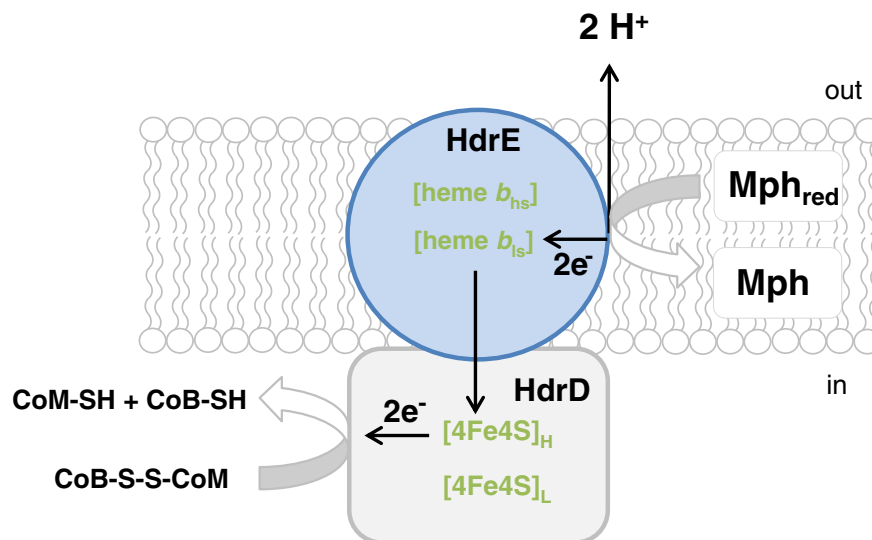
Fig. 9. Simplified scheme of the HdrDE-type heterodisulfide reductase. Direct involvement of electron transport was demonstrated for the low-spin heme (heme b_{ls}) but not for the high-spin heme (heme b_{hs}). The high potential FeS cluster ($[4Fe4S]_H$) was also demonstrated to be involved in electron transport whereas the other, low potential FeS cluster ($[4Fe4S]_L$) is involved in the stabilization of the thiyl intermediate that is formed during catalysis. For more details, see text. Blue colour indicates the membrane integral cytochrome b subunit.

dikinase from *Thermoproteus tenax* [28,187]. This protein catalyzes the reversible reaction between pyruvate, ATP and phosphate to phospho-enolpyruvate, AMP and pyrophosphate. This reaction is part of the central carbon metabolism and could provide a less costly route of interconversion of central carbon metabolites. It can, however, not account for the majority of PP_i turnover from the acetate activation reaction because the flux of substrate through the methanogenic pathway is by far greater than the biosynthetic need for central carbon metabolites. As to the current state of our knowledge it can be assumed that the vast amount of the PP_i generated in the acetate activation reaction of *Methanosaeta* species is indeed hydrolyzed by a soluble pyrophosphatase and that the free energy change associated with the hydrolysis of the P–P anhydrous bond ($\Delta G^{0\prime} = -20$ kJ/mol [188]) is dissipated as heat.

During methane production from acetyl-CoA in *Methanosaeta* species, Fd is reduced and CoM-S-S-CoB is produced (Fig. 2). As described in Section 4.3 Fd_{red} is the electron donor to the membrane bound *Mt. thermophila* electron transport chain [33] that leads to the reduction of the heterodisulfide [33] (Fig. 10A). Other electron donors, e.g. H_2, $F_{420}H_2$ or NADH are not oxidized by *Mt. thermophila* membrane fractions [33]. Regarding the identity of the terminal reductase, an HdrDE-type membrane bound heterodisulfide reductase is encoded in all sequenced *Methanosaeta* genomes [30–32] indicating that this enzyme forms the terminal reductase of the electron transport chain. In contrast, the identity of the Fd_{red} oxidizing enzyme complex is puzzling. The *Mt. thermophila* genome neither contains genes for an Ech hydrogenase nor for an Rnf complex. The same is true for the genomes of *Mt. harundinacea* [31] and *Mt. concilii* [32]. However, Ech hydrogenase and the Rnf complex are the only two membrane complexes known in methanogens that oxidize Fd_{red}. Instead, all *Methanosaeta* genomes contain genes encoding an $F_{420}H_2$ dehydrogenase (*fpoABCDHIJKLMNO*) without the $F_{420}H_2$-oxidizing subunit FpoF. The lack of FpoF leads to the inability of the *Mt. thermophila* membrane fraction to oxidize cofactor $F_{420}H_2$ (Fig. 10A) [33]. It was demonstrated that the *fpo* operon is

highly transcribed in *Mt. thermophila* (unpublished results) indicating an important function in metabolism. These findings led to the idea that the incomplete $F_{420}H_2$ dehydrogenase could be involved in Fd-dependent electron transport. Two possibilities exist how the $F_{420}H_2$ dehydrogenase could contribute to Fd_{red} oxidation: (i) in *Mt. thermophila* there is another yet unknown electron input subunit that productively works with the core complex FpoA-O and is encoded elsewhere in the chromosome. (ii) The core enzyme FpoA-O is catalytically active without FpoF or other subunits channelling electrons directly into the complex. Hence, the truncated complex would accept electrons directly from Fd_{red} without the need of an alternative electron input subunit. In agreement with this idea is the hypothesis that some complex I homologues in cyanobacteria and chloroplasts that do not contain Nqo1, 2, and 3 homologues use Fd_{red} as electron donor [189–191].

In archaea other than *Methanosarcina*, complex I homologues have hardly been investigated but are widely distributed. However, archaeal genomes always lack Nqo1, 2, and 3 [138]. Obviously the evolutionary event of the acquisition of *nqo*1, 2, and 3 happened after the separation of bacteria and archaea. Methanogens and *Archaeoglobus* species are the only archaea that utilize FpoF (or FqoF in *Archaeoglobus*) as replacement for Nqo1, 2, and 3 and as an electron input subunit for $F_{420}H_2$ [192–194]. For the other archaea, however, no electron input protein has been found and the functioning of complex I homologues remains unclear. In light of the nature of the electron donor of the respective respiratory systems it is noteworthy that Fd is ubiquitous in archaea and that many archaea rely on Fd-dependent enzymes instead of enzymes that use NAD^+/NADH as cofactor. Biochemical investigations revealed a huge number of 2-oxoacid: Fd oxidoreductases, aldehyde: Fd oxidoreductases and glyceraldehyde: Fd oxidoreductase in archaea [195–201]. Therefore, it seems feasible that the truncated complex I of archaea serves as Fd: quinone oxidoreductase. This is consistent with the hypothesis that *Mt. thermophila* uses the truncated complex I homologue Fpo for Fd_{red} oxidation as described above. Fd could transfer electrons to the iron–sulfur clusters in either FpoB or FpoI. When FpoI
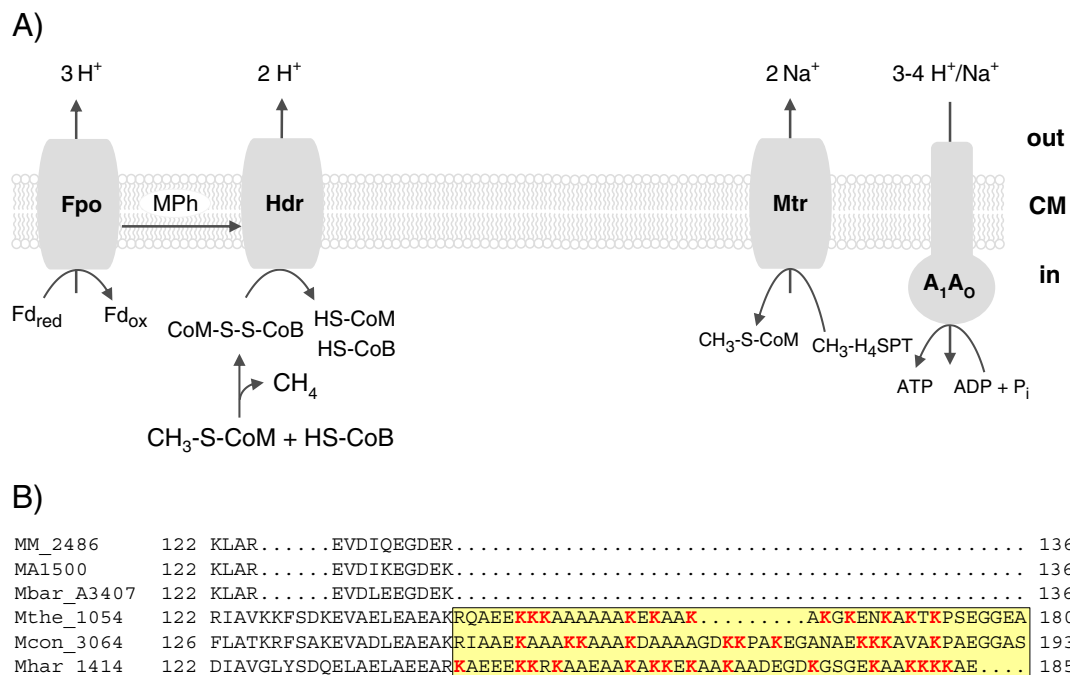
Fig. 10. Process of energy conservation in *Methanosaeta* species. (A) Model of electron transport and ion translocation during aceticlastic growth of *Mt. thermophila*. Fpo, $F_{420}H_2$ dehydrogenase without input module FpoF; Hdr, heterodisulfide reductase; Mtr, methyl-H_4SPT–coenzyme M methyltransferase; A_1A_O, ATP synthase. (B) Alignment of FpoI homologues of different methanogenic archaea. FpoI of *Methanosaeta* sp. contain a C-terminal extension with an accumulation of basic lysine residues. MM_2486, *Ms. mazei* NP_634510.1 (the corresponding gene in the database contains a wrong start codon. In the alignment, the correct start amino acid further downstream was chosen); MA1500, *Ms. acetivorans* NP_616434.1; Mbar_A3407, *Ms. barkeri* YP_306860.1; Mthe_1054, *Mt. thermophila* YP_843478.1; Mcon_3064, *Mt. concilii* YP_004385202.1; Mhar_1414, *Mt. harundinacea* YP_005920401.1.

homologues of different *Methanosarcina* and *Methanosaeta* species were compared it became apparent that the FpoI subunit of *Mt. harundinacea*, *Mt. concilii* and *Mt. thermophila* is modified: in these organisms FpoI contains a C-terminal extension with an accumulation of lysine residues (Fig. 10B). Lysine is a basic amino acid and the basic C-terminal extension could facilitate the interaction with the acidic Fd.

If the $F_{420}H_2$ dehydrogenase in *Methanosaeta* species uses Fd_{red} as electron acceptor severe consequences on the efficiency of ion translocation can be postulated. The redox potential of Fd_{red}, produced by the acetyl-CoA synthetase/CO dehydrogenase, should be around -500 mV [34] leading to a $\Delta E^{0\prime}$ of 335 mV between Fd_{red} and the acceptor Mph ($\Delta E^{0\prime} = -165$ mV [48]). Thermodynamical maximum of translocated protons is above 3. Hence, with Fd_{red} as electron donor $F_{420}H_2$ dehydrogenase could translocate $3H^+/2e^-$. As described in Section 5.3 the $F_{420}H_2$ dehydrogenase is According to Eq. (7) the very similar to complex I and probably comprises four potential H^+ transloacting channels (three antiporter-like subunits and the E-channel) one of which might be nonfunctional (FpoL) because of an insertion in TM12 (Section 5.3). Interestingly, in *Methanosaeta* species subunit FpoL does not contain such an insertion (Fig. 8) and it can be assumed that proton translocation at this coupling site might be possible. Hence, we can speculate that with Fd_{red} a maximum of three of the coupling sites are in action (Figs. 7 and 10) whereas with $F_{420}H_2$ only two would be engaged (Figs. 3 and 7).

Regarding the energy balance of the whole respiratory process in *Mt. thermophila*, we take into account $3H^+/2e^-$ translocated by $F_{420}H_2$ dehydrogenase, $2H^+/2e^-$ translocated by the heterodisulfide reductase during the oxidation of Mph_{red} coupled to the reduction of the heterodisulfide and 2 Na^+ translocated during the methyl transferase reaction (Fig. 10). In total, the number would add up to seven translocated ions during the breakdown of one acetate molecule. Estimating that the ATP synthase is bi-functional as shown for that of the relative *Ms. acetivorans* [78] and functions with a stoichiometry of 3 ions per ADP phosphorylation, 2 ATP molecules and one extra translocated ion would be provided from one acetate molecule. Taking into account the initial activation reaction of acetate in *Methanosaeta* species that was shown to hydrolyze two ATP equivalents, it can be estimated that three mole acetate are needed to phosphorylate one mole of ADP to ATP. The extrusion of only one extra ion per breakdown of a substrate molecule is the minimal energy quantum to sustain life [202], so *Methanosaeta* species really thrive at the energetical limit but are nevertheless able to survive. In summary, these archaeal organisms evolved very sophisticated mechanisms to conserve even very little energy increments. Hence, *Methanosaeta* species are suitable models to investigate the principal mechanisms of how cells synthesize ATP under extreme energy limitation. Members of the genus *Methanosarcina* also translocate about 7 ions per acetate molecule (Fig. 4A/B): $1H^+/2e^-$ by Ech hydrogenase [95], $2H^+$ by the Mph-reducing hydrogenase [84] (or 3 $Na^+/2e^-$ in *Ms. acetivorans* by Rnf [97]), $2H^+/2e^-$ by the heterodisulfide reductase [84] and 2 Na^+ by the methyl transferase [61]. Taking into account a maximal stoichiometry of the ATP synthase of 4 Na^+/H^+ per ADP phosphorylation [78] 1.75 ATP can be synthesized. However, the acetate activation reaction in *Methanosarcina* species only requires one mole ATP per mole acetate. Hence, the final energy yield is higher as compared to *Methanosaeta*. This is reflected in the growth yields of *Methanosarcina* and *Methanosaeta* species that are in the range of 3.0 g/mol acetate and 1.4 g/mol acetate, respectively [29,203,204]. On the other hand, *Methanosaeta* species require a lower minimal acetate concentration for growth [29] enabling them to thrive in ecological niches that contain very low amounts of acetate.

References

[1] J.G. Ferry, Fundamentals of methanogenic pathways that are key to the biomethanation of complex biomass, Curr. Opin. Biotechnol. 22 (2011) 351–357.

[2] M. Morita, K. Sasaki, Factors influencing the degradation of garbage in methanogenic bioreactors and impacts on biogas formation, Appl. Microbiol. Biotechnol. 94 (2012) 575–582.

[3] J.L. Garcia, B.K. Patel, B. Ollivier, Taxonomic, phylogenetic, and ecological diversity of methanogenic archaea, Anaerobe 6 (2000) 205–226.

[4] B. Schink, Energetics of syntrophic cooperation in methanogenic degradation, Microbiol. Mol. Biol. Rev. 61 (1997) 262–280.

[5] M.J. McInerney, J.R. Sieber, R.P. Gunsalus, Syntrophy in anaerobic global carbon cycles, Curr. Opin. Biotechnol. 20 (2009) 623–632.

[6] A.J. Stams, C.M. Plugge, Electron transfer in syntrophic communities of anaerobic bacteria and archaea, Nat. Rev. Microbiol. 7 (2009) 568–577.

[7] U. Deppenmeier, The unique biochemistry of methanogenesis, Prog. Nucleic Acid Res. Mol. Biol. 71 (2002) 223–283.

[8] R.K. Thauer, A.K. Kaster, M. Goenrich, M. Schick, T. Hiromoto, S. Shima, Hydrogenases from methanogenic archaea, nickel, a novel cofactor, and H_2 storage, Ann. Rev. Biochem. 79 (2010) 507–536.

[9] Y. Liu, W.B. Whitman, Metabolic, phylogenetic, and ecological diversity of the methanogenic archaea, Ann. N. Y. Acad. Sci. 1125 (2008) 171–189.

[10] J.R. Marchesi, A.J. Weightman, B.A. Cragg, R.J. Parkes, J.C. Fry, Methanogen and bacterial diversity and distribution in deep gas hydrate sediments from the Cascadia Margin as revealed by 16S rRNA molecular analysis, FEMS Microbiol. Ecol. 34 (2001) 221–228.

[11] W.J. Winters, S.R. Dallimore, T.S. Collett, K.A. Jenner, J.T. Katsube, R.E. Cranston, J.F. Wright, F.M. Nixon, T. Uchida, Relation between gas hydrate and physical properties at the Mallik 2 L-38 research well in the Mackenzie Delta, Ann. N. Y. Acad. Sci. 912 (2000) 94–100.

[12] C.D. Ruppel, Methane hydrates and contemporary climate change, Nat. Educ. Knowl. 3 (2011) 29.

[13] C. Welte, U. Deppenmeier, Blackbox für Biogas, LaborPraxis 37 (2013) 14–16.

[14] K. Paul, J.O. Nonoh, L. Mikulski, A. Brune, "Methanoplasmatales," Thermoplasmatales-related archaea in termite guts and other environments, are the seventh order of methanogens, Appl. Environ. Microbiol. 78 (2012) 8245–8253.

[15] S.H. Zinder, Physiological ecology of methanogens, in: J.G. Ferry (Ed.), Methanogenesis, Chapman & Hall, New York-London, 1993, pp. 128–206.

[16] W. Buckel, R.K. Thauer, Energy conservation via electron bifurcating ferredoxin reduction and proton/Na^+ translocating ferredoxin oxidation, Biochim. Biophys. Acta 1827 (2013) 94–113.

[17] J.G. Ferry, Enzymology of one-carbon metabolism in methanogenic pathways, FEMS Microbiol. Rev. 23 (1999) 13–38.

[18] R.K. Thauer, Biochemistry of methanogenesis: a tribute to Marjory Stephenson, Microbiology 144 (1998) 2377–2406.

[19] U. Deppenmeier, Redox-driven proton translocation in methanogenic archaea, Cell. Mol. Life Sci. 59 (2002) 1513–1533.

[20] J.G. Ferry, How to make a living by exhaling methane, Ann. Rev. Microbiol. 64 (2010) 453–473.

[21] D.R. Boone, W.B. Whitman, P.E. Rouvière, Diversity and taxonomy of methanogens, in: J.G. Ferry (Ed.), Methanogenesis, Chapman & Hall, New York, 1993, pp. 35–80.

[22] L.E. Mayerhofer, A.J. Macario, E.C. de Macario, Lamina, a novel multicellular form of *Methanosarcina mazei* S-6, J. Bacteriol. 174 (1992) 309–314.

[23] U. Deppenmeier, A. Johann, T. Hartsch, R. Merkl, R.A. Schmitz, R. Martinez-Arias, A. Henne, A. Wiezer, S. Bäumer, C. Jacobi, H. Brüggemann, T. Lienard, A. Christmann, M. Bomeke, S. Steckel, A. Bhattacharyya, A. Lykidis, R. Overbeek, H.P. Klenk, R.P. Gunsalus, H.J. Fritz, G. Gottschalk, The genome of *Methanosarcina mazei*: evidence for lateral gene transfer between bacteria and archaea, J. Mol. Microbiol. Biotechnol. 4 (2002) 453–461.

[24] J.E. Galagan, C. Nusbaum, A. Roy, M.G. Endrizzi, P. Macdonald, W. FitzHugh, S. Calvo, R. Engels, S. Smirnov, D. Atnoor, A. Brown, N. Allen, J. Naylor, N. Stange-Thomann, K. DeArellano, R. Johnson, L. Linton, P. McEwan, K. McKernan, J. Talamas, A. Tirrell, W. Ye, A. Zimmer, R.D. Barber, I. Cann, D.E. Graham, D.A. Grahame, A.M. Guss, R. Hedderich, C. Ingram-Smith, H.C. Kuettner, J.A. Krzycki, J.A. Leigh, W. Li, J. Liu, B. Mukhopadhyay, J.N. Reeve, K. Smith, T.A. Springer, L.A. Umayam, O. White, R.H. White, E. Conway de Macario, J.G. Ferry, K.F. Jarrell, H. Jing, A.J. Macario, I. Paulsen, M. Pritchett, K.R. Sowers, R.V. Swanson, S.H. Zinder, E. Lander, W.W. Metcalf, B. Birren, The genome of *M. acetivorans* reveals extensive metabolic and physiological diversity, Genome Res. 12 (2002) 532–542.

[25] D.L. Maeder, I. Anderson, T.S. Brettin, D.C. Bruce, P. Gilna, C.S. Han, A. Lapidus, W.W. Metcalf, E. Saunders, R. Tapia, K.R. Sowers, The *Methanosarcina barkeri* genome: comparative analysis with *Methanosarcina acetivorans* and *Methanosarcina mazei* reveals extensive rearrangement within methanosarcinal genomes, J. Bacteriol. 188 (2006) 7922–7931.

[26] S. Nelson-Sathi, T. Dagan, G. Landan, A. Janssen, M. Steel, J.O. McInerney, U. Deppenmeier, W.F. Martin, Acquisition of 1,000 eubacterial genes physiologically transformed a methanogen at the origin of Haloarchaea, Proc. Natl. Acad. Sci. U. S. A. 109 (2012) 20537–20542.

[27] B.A. Huser, K. Wuhrmann, A.J.B. Zehnder, *Methanothrix soehngenii gen. nov. sp. nov.*, a new acetotrophic non-hydrogen-oxidizing methane bacterium, Arch. Microbiol. 132 (1982) 1–9.

[28] S. Berger, C. Welte, U. Deppenmeier, Acetate activation in *Methanosaeta thermophila*: characterization of the key enzymes pyrophosphatase and acetyl-CoA synthetase, Archaea 2012 (2012) 315153.

[29] M.S.M. Jetten, A.J.M. Stams, A.J.B. Zehnder, Methanogenesis from acetate —a comparison of the acetate metabolism in *Methanothrix soehngenii* and *Methanosarcina* spp. FEMS Microbiol. Rev. 88 (1992) 181–197.

[30] K.S. Smith, C. Ingram-Smith, *Methanosaeta*, the forgotten methanogen? Trends Microbiol. 15 (2007) 150–155.

[31] J. Zhu, H. Zheng, G. Ai, G. Zhang, D. Liu, X. Liu, X. Dong, The genome characteristics and predicted function of methyl-group oxidation pathway in the obligate aceticlastic methanogens, *Methanosaeta* spp. PloS ONE 7 (2012) e36756.

[32] R.D. Barber, L. Zhang, M. Harnack, M.V. Olson, R. Kaul, C. Ingram-Smith, K.S. Smith, Complete genome sequence of *Methanosaeta concilii*, a specialist in aceticlastic methanogenesis, J. Bacteriol. 193 (2011) 3668–3669.

[33] C. Welte, U. Deppenmeier, Membrane-bound electron transport in *Methanosaeta thermophila*, J. Bacteriol. 193 (2011) 2868–2870.

[34] R.K. Thauer, A.K. Kaster, H. Seedorf, W. Buckel, R. Hedderich, Methanogenic archaea: ecologically relevant differences in energy conservation, Nat. Rev. Microbiol. 6 (2008) 579–591.

[35] U. Deppenmeier, V. Müller, Life close to the thermodynamic limit: how methanogenic archaea conserve energy, Results Probl. Cell Differ. 45 (2008) 123–152.

[36] M.A. Gaston, R. Jiang, J.A. Krzycki, Functional context, biosynthesis, and genetic encoding of pyrrolysine, Curr. Opin. Microbiol. 14 (2011) 342–349.

[37] R.S. Wolfe, Unusual coenzymes of methanogenesis, Trends Biochem. Sci. 10 (1985) 396–399.

[38] H.C. Friedmann, A. Klein, R.K. Thauer, Structure and function of the nickel porphinoid, coenzyme F_{430} and of its enzyme, methyl coenzyme M reductase, FEMS Microbiol. Rev. 7 (1990) 339–348.

[39] U. Ermler, n the mechanism of methyl-coenzyme M reductase, Dalton Trans. (2005) 3451–3458.

[40] U. Ermler, W. Grabarse, S. Shima, M. Goubeaud, R.K. Thauer, Crystal structure of methyl-coenzyme M reductase: the key enzyme of biological methane formation, Science 278 (1997) 1457–1462.

[41] D.A. Livingston, A. Pfaltz, J. Schreiber, A. Eschenmoser, D. Ankelfuchs, J. Moll, R. Jaenchen, R.K. Thauer, Factor F_{430} from methanogenic bacteria - structure of the protein-free factor, Helv. Chim. Acta 67 (1984) 334–351.

[42] R.K. Thauer, Enzymology —nickel to the fore, Science 293 (2001) 1264–1265.

[43] C. Walsh, Naturally occurring 5-deazaflavin coenzymes —biological redox roles, Acc. Chem. Res. 19 (1986) 216–221.

[44] K.M. Noll, K.L. Rinehart, R.S. Tanner, R.S. Wolfe, Structure of component-B (7-mercaptoheptanoylthreonine phosphate) of the methylcoenzyme M methylreductase system of *Methanobacterium thermoautotrophicum*, Proc. Natl. Acad. Sci. U. S. A. 83 (1986) 4238–4242.

[45] A. Kobelt, A. Pfaltz, D. Ankelfuchs, R.K. Thauer, The L-form of *N*-7-mercaptoheptanoyl-*O*-phosphothreonine is the enantiomer active as component B in methyl-CoM reduction to methane, FEBS Lett. 214 (1987) 265–268.

[46] S. Bäumer, T. Ide, C. Jacobi, A. Johann, G. Gottschalk, U. Deppenmeier, The $F_{420}H_2$ dehydrogenase from *Methanosarcina mazei* is a redox-driven proton pump closely related to NADH dehydrogenases, J. Biol. Chem. 275 (2000) 17968–17973.

[47] U. Beifuss, M. Tietze, S. Bäumer, U. Deppenmeier, Methanophenazine: structure, total synthesis, and function of a new cofactor from methanogenic archaea, Angew. Chem. Int. Ed. Engl. 39 (2000) 2470–2472.

[48] M. Tietze, A. Beuchle, I. Lamla, N. Orth, M. Dehler, G. Greiner, U. Beifuss, Redox potentials of methanophenazine and CoB-S-S-CoM, factors involved in electron transport in methanogenic archaea, Chembiochem 4 (2003) 333–335.

[49] J.G. Ferry, Enzymology of the fermentation of acetate to methane by *Methanosarcina thermophila*, Biofactors 6 (1997) 25–35.

[50] M.S. Jetten, T.J. Fluit, A.J. Stams, A.J. Zehnder, A fluoride-insensitive inorganic pyrophosphatase isolated from *Methanothrix soehngenii*, Arch. Microbiol. 157 (1992) 284–289.

[51] M.S. Jetten, A.J. Stams, A.J. Zehnder, Isolation and characterization of acetyl-coenzyme A synthetase from *Methanothrix soehngenii*, J. Bacteriol. 171 (1989) 5430–5435.

[52] Y.L. Teh, S. Zinder, Acetyl-coenzyme A synthetase in the thermophilic, acetate-utilizing methanogen *Methanothrix* sp. strain CALS-1, FEMS Microbiol. Lett. 98 (1992) 1–8.

[53] R.D. Miles, P.P. Iyer, J.G. Ferry, Site-directed mutational analysis of active site residues in the acetate kinase from *Methanosarcina thermophila*, J. Biol. Chem. 276 (2001) 45059–45064.

[54] K.C. Terlesky, M.J.K. Nelson, J.G. Ferry, Isolation of an enzyme complex with carbon monoxide dehydrogenase activity containing corrinoid and nickel from acetate-grown *Methanosarcina thermophila*, J. Bacteriol. 168 (1986) 1053–1058.

[55] D.A. Grahame, Catalysis of acetyl-CoA cleavage and tetrahydrosarcinapterin methylation by a carbon monoxide dehydrogenase corrinoid enzyme complex, J. Biol. Chem. 266 (1991) 22227–22233.

[56] J.G. Ferry, CO dehydrogenase, Ann. Rev. Microbiol. 49 (1995) 305–333.

[57] E. Oelgeschläger, M. Rother, Carbon monoxide-dependent energy metabolism in anaerobic bacteria and archaea, Arch. Microbiol. 190 (2008) 257–269.

[58] W. Gong, B. Hao, Z. Wei, D.J. Ferguson, T. Tallant, J.A. Krzycki, M.K. Chan, Structure of the alpha(2)epsilon(2) Ni-dependent CO dehydrogenase component of the *Methanosarcina barkeri* acetyl-CoA decarbonylase/synthase complex, Proc. Natl. Acad. Sci. U. S. A. 105 (2008) 9558–9563.

[59] G. Gottschalk, R.K. Thauer, The Na^+-translocating methyltransferase complex from methanogenic archaea, Biochim. Biophys. Acta 1505 (2001) 28–36.

[60] V. Müller, C. Winner, G. Gottschalk, Electron transport driven sodium extrusion during methanogenesis from formaldehyde and molecular hydrogen by *Methanosarcina barkeri*, Eur. J. Biochem. 178 (1988) 519–525.

[61] B. Becher, V. Müller, G. Gottschalk, N^5-methyl-tetrahydromethanopterin:coenzyme M methyltransferase of *Methanosarcina strain* Gö1 is an Na^+-translocating membrane protein, J. Bacteriol. 174 (1992) 7656–7660.

[62] T.A. Bobik, K.D. Olson, K.M. Noll, R.S. Wolfe, Evidence that the heterodisulfide of coenzyme M and 7-mercaptoheptanoylthreonine phosphate is a product of the methylreductase reaction in *Methanobacterium*, Biochem. Biophys. Res. Commun. 149 (1987) 455–460.

[63] J. Ellermann, R. Hedderich, R. Böcher, R.K. Thauer, The final step in methane formation. Investigations with highly purified methyl-CoM reductase (component C) from *Methanobacterium thermoautotrophicum* (strain Marburg), Eur. J. Biochem. 172 (1988) 669–677.

[64] J.A. Krzycki, Function of genetically encoded pyrrolysine in corrinoid-dependent methylamine methyltransferases, Curr. Opin. Chem. Biol. 8 (2004) 484–491.

[65] P.A. Bertram, R.K. Thauer, Thermodynamics of the formylmethanofuran dehydrogenase reaction in *Methanobacterium thermoautotrophicum*, Eur. J. Biochem. 226 (1994) 811–818.

[66] R. Michel, C. Massanz, S. Kostka, M. Richter, K. Fiebig, Biochemical characterization of the 8-hydroxy-5-deazaflavin-reactive hydrogenase from *Methanosarcina barkeri* Fusaro, Eur. J. Biochem. 233 (1995) 727–735.

[67] F. Li, J. Hinderberger, H. Seedorf, J. Zhang, W. Buckel, R.K. Thauer, Coupled ferredoxin and crotonyl coenzyme A (CoA) reduction with NADH catalyzed by the butyryl-CoA dehydrogenase/Etf complex from *Clostridium kluyveri*, J. Bacteriol. 190 (2008) 843–850.

[68] A.K. Kaster, J. Moll, K. Parey, R.K. Thauer, Coupling of ferredoxin and heterodisulfide reduction via electron bifurcation in hydrogenotrophic methanogenic archaea, Proc. Natl. Acad. Sci. U. S. A. 108 (2011) 2981–2986.

[69] K.C. Costa, P.M. Wong, T. Wang, T.J. Lie, J.A. Dodsworth, I. Swanson, J.A. Burn, M. Hackett, J.A. Leigh, Protein complexing in a methanogen suggests electron bifurcation and electron delivery from formate to heterodisulfide reductase, Proc. Natl. Acad. Sci. U. S. A. 107 (2010) 11050–11055.

[70] K.C. Costa, T.J. Lie, Q. Xia, J.A. Leigh, VhuD facilitates electron flow from H_2 or formate to heterodisulfide reductase in *Methanococcus maripaludis*, J. Bacteriol. 195 (2013) 5160–5165.

[71] T. Lienard, B. Becher, M. Marschall, S. Bowien, G. Gottschalk, Sodium ion translocation by N^5-methyltetrahydromethanopterin: coenzyme M methyltransferase from *Methanosarcina mazei* Gö1 reconstituted in ether lipid liposomes, Eur. J. Biochem. 239 (1996) 857–864.

[72] K. Schlegel, V. Müller, Evolution of Na^+ and H^+ bioenergetics in methanogenic archaea, Biochem. Soc. Trans. 41 (2013) 421–426.

[73] J.G. Ferry, The chemical biology of methanogenesis, Planet. Space Sci. 58 (2010) 1775–1783.

[74] V. Müller, T. Lemker, A. Lingl, C. Weidner, U. Coskun, G. Grüber, Bioenergetics of archaea: ATP synthesis under harsh environmental conditions, J. Mol. Microbiol. Biotechnol. 10 (2005) 167–180.

[75] V. Müller, G. Grüber, ATP synthases: structure, function and evolution of unique energy converters, Cell. Mol. Life Sci. 60 (2003) 474–494.

[76] R.L. Cross, V. Müller, The evolution of A-, F-, and V-type ATP synthases and ATPases: reversals in function and changes in the H^+/ATP coupling ratio, FEBS Lett. 576 (2004) 1–4.

[77] V. Müller, A. Lingl, K. Lewalter, M. Fritz, ATP synthases with novel rotor subunits: new insights into structure, function and evolution of ATPases, J. Bioenerg. Biomembr. 37 (2005) 455–460.

[78] K. Schlegel, V. Leone, J.D. Faraldo-Gómez, V. Müller, Promiscuous archaeal ATP synthase concurrently coupled to Na^+ and H^+ translocation, Proc. Natl. Acad. Sci. U. S. A. 109 (2012) 947–952.

[79] R. Jasso-Chavez, E.E. Apolinario, K.R. Sowers, J.G. Ferry, MrpA functions in energy conversion during acetate-dependent growth of *Methanosarcina acetivorans*, J. Bacteriol. 195 (2013) 3987–3994.

[80] M. Blaut, G. Gottschalk, Coupling of ATP synthesis and methane formation from methanol and molecular hydrogen in *Methanosarcina barkeri*, Eur. J. Biochem. 141 (1984) 217–222.

[81] S. Peinemann, Kopplung von ATP-Synthese und Methanogenese in Vesikelpräparationen des methanogenen Bakteriums Stamm Gö1, [PhD thesis] Georg-August-Universität Göttingen, Germany, 1989.

[82] V. Müller, M. Blaut, G. Gottschalk, Generation of a transmembrane gradient of Na^+ in *Methanosarcina barkeri*, Eur. J. Biochem. 162 (1987) 461–466.

[83] U. Deppenmeier, M. Blaut, G. Gottschalk, H_2: heterodisulfide oxidoreductase, a 2nd energy-conserving system in the methanogenic strain Gö1, Arch. Microbiol. 155 (1991) 272–277.

[84] T. Ide, S. Bäumer, U. Deppenmeier, Energy conservation by the H_2:heterodisulfide oxidoreductase from *Methanosarcina mazei* Gö1: identification of two proton-translocating segments, J. Bacteriol. 181 (1999) 4076–4080.

[85] U. Deppenmeier, M. Blaut, A. Mahlmann, G. Gottschalk, Reduced coenzyme F_{420}: heterodisulfide oxidoreductase, a proton- translocating redox system in methanogenic bacteria, Proc. Natl. Acad. Sci. U. S. A. 87 (1990) 9449–9453.

[86] C. Welte, U. Deppenmeier, Re-evaluation of the function of the F_{420} dehydrogenase in electron transport in *Methanosarcina mazei*, FEBS J. 278 (2011) 1277–1287.

[87] G. Kulkarni, D.M. Kridelbaugh, A.M. Guss, W.W. Metcalf, Hydrogen is a preferred intermediate in the energy-conserving electron transport chain of *Methanosarcina barkeri*, Proc. Natl. Acad. Sci. U. S. A. 106 (2009) 15915–15920.

[88] F.M. Harald, The Vital Force: A Study of Bioenergetics, W.H. Freeman and Company, New York, 1986.

[89] R.K. Thauer, S. Shima, Methane as fuel for anaerobic microorganisms, Ann. N. Y. Acad. Sci. 1125 (2008) 158–170.

[90] J.A. Vorholt, M. Vaupel, R.K. Thauer, A polyferredoxin with eight [4Fe-4S] clusters as a subunit of molybdenum formylmethanofuran dehydrogenase from Methanosarcina barkeri, Eur. J. Biochem. 236 (1996) 309–317.

[91] R. Fischer, R.K. Thauer, Ferredoxin-dependent methane formation from acetate in cell extracts of Methanosarcina barkeri (strain MS), FEBS Lett. 269 (1990) 368–372.

[92] J. Meuer, H.C. Kuettner, J.K. Zhang, R. Hedderich, W.W. Metcalf, Genetic analysis of the archaeon Methanosarcina barkeri Fusaro reveals a central role for Ech hydrogenase and ferredoxin in methanogenesis and carbon fixation, Proc. Natl. Acad. Sci. U. S. A. 99 (2002) 5632–5637.

[93] J. Meuer, S. Bartoschek, J. Koch, A. Künkel, R. Hedderich, Purification and catalytic properties of Ech hydrogenase from Methanosarcina barkeri, Eur. J. Biochem. 265 (1999) 325–335.

[94] C. Welte, V. Kallnik, M. Grapp, G. Bender, S. Ragsdale, U. Deppenmeier, Function of Ech hydrogenase in ferredoxin-dependent, membrane-bound electron transport in Methanosarcina mazei, J. Bacteriol. 192 (2010) 674–678.

[95] C. Welte, C. Krätzer, U. Deppenmeier, Involvement of Ech hydrogenase in energy conservation of Methanosarcina mazei, FEBS J. 277 (2010) 3396–3403.

[96] M. Wang, J.F. Tomb, J.G. Ferry, Electron transport in acetate-grown Methanosarcina acetivorans, BMC Microbiol. 11 (2011) 165.

[97] K. Schlegel, C. Welte, U. Deppenmeier, V. Müller, Electron transport during aceticlastic methanogenesis by Methanosarcina acetivorans involves a sodium-translocating Rnf complex, FEBS J. 279 (2012) 4444–4452.

[98] M. Bott, R.K. Thauer, Proton translocation coupled to the oxidation of carbon monoxide to CO_2 and H_2 in Methanosarcina barkeri, Eur. J. Biochem. 179 (1989) 469–472.

[99] A. Tersteegen, R. Hedderich, Methanobacterium thermoautotrophicum encodes two multisubunit membrane-bound [NiFe] hydrogenases. Transcription of the operons and sequence analysis of the deduced proteins, Eur. J. Biochem. 264 (1999) 930–943.

[100] D.A. Grahame, E. DeMoll, Substrate and accessory protein requirements and thermodynamics of acetyl-CoA synthesis and cleavage in Methanosarcina barkeri, Biochemistry 34 (1995) 4617–4624.

[101] A.K. Bock, J. Kunow, J. Glasemacher, P. Schönheit, Catalytic properties, molecular composition and sequence alignments of pyruvate:ferredoxin oxidoreductase from the methanogenic archaeon Methanosarcina barkeri (strain Fusaro), Eur. J. Biochem. 237 (1996) 35–44.

[102] R. Hedderich, L. Forzi, Energy-converting [NiFe] hydrogenases: more than just H_2 activation, J. Mol. Microbiol. Biotechnol. 10 (2005) 92–104.

[103] J.G. Ferry, D.J. Lessner, Methanogenesis in marine sediments, Ann. N. Y. Acad. Sci. 1125 (2008) 147–157.

[104] A.M. Guss, B. Mukhopadhyay, J.K. Zhang, W.W. Metcalf, Genetic analysis of mch mutants in two Methanosarcina species demonstrates multiple roles for the methanopterin-dependent C_1 oxidation/reduction pathway and differences in H_2 metabolism between closely related species, Mol. Microbiol. 55 (2005) 1671–1680.

[105] Q. Li, L. Li, T. Rejtar, D.J. Lessner, B.L. Karger, J.G. Ferry, Electron transport in the pathway of acetate conversion to methane in the marine archaeon Methanosarcina acetivorans, J. Bacteriol. 188 (2006) 702–710.

[106] A.M. Guss, G. Kulkarni, W.W. Metcalf, Differences in hydrogenase gene expression between Methanosarcina acetivorans and Methanosarcina barkeri, J. Bacteriol. 191 (2009) 2826–2833.

[107] L. Rohlin, R.P. Gunsalus, Carbon-dependent control of electron transfer and central carbon pathway genes for methane biosynthesis in the Archaean, Methanosarcina acetivorans strain C2A, BMC Microbiol. 10 (2010) 62.

[108] E. Biegel, V. Müller, Bacterial Na^+-translocating ferredoxin:NAD^+ oxidoreductase, Proc. Natl. Acad. Sci. U. S. A. 107 (2010) 18138–18142.

[109] V. Hess, K. Schuchmann, V. Müller, The ferredoxin:NAD^+ oxidoreductase (Rnf) from the acetogen Acetobacterium woodii requires Na^+ and is reversibly coupled to the membrane potential, J. Biol. Chem. 288 (2013)[31496-13502].

[110] P.M. Vignais, B. Billoud, Occurrence, classification, and biological function of hydrogenases: an overview, Chem. Rev. 107 (2007) 4206–4272.

[111] J.C. Fontecilla-Camps, P. Amara, C. Cavazza, Y. Nicolet, A. Volbeda, Structure-function relationships of anaerobic gas-processing metalloenzymes, Nature 460 (2009) 814–822.

[112] J.C. Fontecilla-Camps, A. Volbeda, C. Cavazza, Y. Nicolet, Structure/function relationships of [NiFe]- and [FeFe]-hydrogenases, Chem. Rev. 107 (2007) 4273–4303.

[113] A. Volbeda, M.H. Charon, C. Piras, E.C. Hatchikian, M. Frey, J.C. Fontecilla-Camps, Crystal structure of the nickel-iron hydrogenase from Desulfovibrio gigas, Nature 373 (1995) 580–587.

[114] M. Vaupel, R.K. Thauer, Two F_{420}-reducing hydrogenases in Methanosarcina barkeri, Arch. Microbiol. 169 (1998) 201–205.

[115] U. Deppenmeier, M. Blaut, B. Schmidt, G. Gottschalk, Purification and properties of a F_{420}-nonreactive, membrane-bound hydrogenase from Methanosarcina strain Gö1, Arch. Microbiol. 157 (1992) 505–511.

[116] J.M. Kemner, J.G. Zeikus, Purification and characterization of membrane-bound hydrogenase from Methanosarcina barkeri MS, Arch. Microbiol. 161 (1994) 47–54.

[117] U. Deppenmeier, Different structure and expression of the operons encoding the membrane-bound hydrogenases from Methanosarcina mazei Gö1, Arch. Microbiol. 164 (1995) 370–376.

[118] B. Kamlage, M. Blaut, Characterization of cytochromes from Methanosarcina strain Gö1 and their involvement in electron transport during growth on methanol, J. Bacteriol. 174 (1992) 3921–3927.

[119] J.M. Kemner, J.A. Krzycki, R.C. Prince, J.G. Zeikus, Spectroscopic and enzymatic evidence for membrane-bound electron transport carriers and hydrogenase and their relation to cytochrome b function in Methanosarcina barkeri, FEMS Microbiol. Lett. 48 (1987) 267–272.

[120] J. Brodersen, S. Bäumer, H.J. Abken, G. Gottschalk, U. Deppenmeier, Inhibition of membrane-bound electron transport of the methanogenic archaeon Methanosarcina mazei Gö1 by diphenyleneiodonium, Eur. J. Biochem. 259 (1999) 218–224.

[121] K. Eismann, K. Mlejnek, D. Zipprich, M. Hoppert, F. Mayer, Antigenic determinants of the membrane-bound hydrogenase in Alcaligenes eutrophus are exposed toward the periplasm, J. Bacteriol. 177 (1995) 6309–6312.

[122] P.M. Vignais, B. Billoud, J. Meyer, Classification and phylogeny of hydrogenases, FEMS Microbiol. Rev. 25 (2001) 455–501.

[123] F.L. Sousa, T. Thiergart, G. Landan, S. Nelson-Sathi, I.A. Pereira, J.F. Allen, N. Lane, W.F. Martin, Early bioenergetic evolution, Philos. Trans. R. Soc. Lond. B Biol. Sci. 368 (2013) 20130088.

[124] J.D. Fox, R.L Kerby, G.P. Roberts, P.W. Ludden, Characterization of the CO-induced, CO-tolerant hydrogenase from Rhodospirillum rubrum and the gene encoding the large subunit of the enzyme, J. Bacteriol. 178 (1996) 1515–1524.

[125] B. Soboh, D. Linder, R. Hedderich, Purification and catalytic properties of a CO-oxidizing:H_2-evolving enzyme complex from Carboxydothermus hydrogenoformans, Eur. J. Biochem. 269 (2002) 5712–5721.

[126] R. Böhm, M. Sauter, A. Böck, Nucleotide sequence and expression of an operon in Escherichia coli coding for formate hydrogenlyase components, Mol. Microbiol. 4 (1990) 231–243.

[127] M. Sauter, R. Böhm, A. Böck, Mutational analysis of the operon hyc determining hydrogenase 3 formation in Escherichia coli, Mol. Microbiol. 6 (1992) 1523–1532.

[128] R. Sapra, K. Bagramyan, M.W. Adams, A simple energy-conserving system: proton reduction coupled to proton translocation, Proc. Natl. Acad. Sci. U. S. A. 100 (2003) 7545–7550.

[129] R. Hovey, S. Lentes, A. Ehrenreich, K. Salmon, K. Saba, G. Gottschalk, R.P. Gunsalus, U. Deppenmeier, DNA microarray analysis of Methanosarcina mazei Gö1 reveals adaptation to different methanogenic substrates, Mol. Genet. Genomics 273 (2005) 225–239.

[130] S. Kurkin, J. Meuer, J. Koch, R. Hedderich, S.P. Albracht, The membrane-bound [NiFe]-hydrogenase (Ech) from Methanosarcina barkeri: unusual properties of the iron-sulphur clusters, Eur. J. Biochem. 269 (2002) 6101–6111.

[131] L. Forzi, J. Koch, A.M. Guss, C.G. Radosevich, W.W. Metcalf, R. Hedderich, Assignment of the [4Fe-4S] clusters of Ech hydrogenase from Methanosarcina barkeri to individual subunits via the characterization of site-directed mutants, FEBS J. 272 (2005) 4741–4753.

[132] A. Künkel, J.A. Vorholt, R.K. Thauer, R. Hedderich, An Escherichia coli hydrogenase-3-type hydrogenase in methanogenic archaea, Eur. J. Biochem. 252 (1998) 467–476.

[133] R. Hedderich, Energy-converting [NiFe] hydrogenases from archaea and extremophiles: ancestors of complex I, J. Bioenerg. Biomembr. 36 (2004) 65–75.

[134] M. Bott, B. Eikmanns, R.K. Thauer, Coupling of carbon monoxide oxidation to CO_2 and H_2 with the phosphorylation of ADP in acetate-grown Methanosarcina barkeri, Eur. J. Biochem. 159 (1986) 393–398.

[135] A. Stojanowic, R. Hedderich, CO_2 reduction to the level of formylmethanofuran in Methanosarcina barkeri is non-energy driven when CO is the electron donor, FEMS Microbiol. Lett. 235 (2004) 163–167.

[136] R.G. Efremov, L.A. Sazanov, The coupling mechanism of respiratory complex I —a structural and evolutionary perspective, Biochim. Biophys. Acta 1817 (2012) 1785–1795.

[137] T. Friedrich, H. Weiss, Modular evolution of the respiratory NADH:ubiquinone oxidoreductase and the origin of its modules, J. Theor. Biol. 187 (1997) 529–540.

[138] V.K. Moparthi, C. Hägerhäll, The evolution of respiratory chain complex I from a smaller last common ancestor consisting of 11 protein subunits, J. Mol. Evol. 72 (2011) 484–497.

[139] B.C. Marreiros, A.P. Batista, A.M. Duarte, M.M. Pereira, A missing link between complex I and group 4 membrane-bound [NiFe] hydrogenases, Biochim. Biophys. Acta 1827 (2013) 198–209.

[140] R.G. Efremov, R. Baradaran, L.A. Sazanov, The architecture of respiratory complex I, Nature 465 (2010) 441–445.

[141] R.G. Efremov, L.A. Sazanov, Structure of the membrane domain of respiratory complex I, Nature 476 (2011) 414–420.

[142] R. Baradaran, J.M. Berrisford, G.S. Minhas, L.A. Sazanov, Crystal structure of the entire respiratory complex I, Nature 494 (2013) 443–448.

[143] N. Kashani-Poor, K. Zwicker, S. Kerscher, U. Brandt, A central functional role for the 49-kDa subunit within the catalytic core of mitochondrial complex I, J. Biol. Chem. 276 (2001) 24082–24087.

[144] J.M. Berrisford, L.A. Sazanov, Structural basis for the mechanism of respiratory complex I, J. Biol. Chem. 284 (2009) 29773–29783.

[145] H. Ogata, W. Lubitz, Y. Higuchi, [NiFe] hydrogenases: structural and spectroscopic studies of the reaction mechanism, Dalton Trans. (2009) 7577–7587.

[146] M. Finel, Does NADH play a central role in energy metabolism in Helicobacter pylori? Trends Biochem. Sci. 23 (1998) 412–413.

[147] M. Schmehl, A. Jahn, A. Meyer zu Vilsendorf, S. Hennecke, B. Masepohl, M. Schuppler, M. Marxer, J. Oelze, W. Klipp, Identification of a new class of nitrogen fixation genes in Rhodobacter capsulatus: a putative membrane complex involved in electron transport to nitrogenase, Mol. Gen. Genet. 241 (1993) 602–615.

[148] F. Imkamp, E. Biegel, E. Jayamani, W. Buckel, V. Müller, Dissection of the caffeate respiratory chain in the acetogen Acetobacterium woodii: identification of an Rnf-type NADH dehydrogenase as a potential coupling site, J. Bacteriol. 189 (2007) 8145–8153.

[149] E. Biegel, S. Schmidt, V. Müller, Genetic, immunological and biochemical evidence for a Rnf complex in the acetogen *Acetobacterium woodii*, Environ. Microbiol. 11 (2009) 1438–1443.

[150] V. Müller, F. Imkamp, E. Biegel, S. Schmidt, S. Dilling, Discovery of a ferredoxin: NAD$^+$-oxidoreductase (Rnf) in *Acetobacterium woodii*: a novel potential coupling site in acetogens, Ann. N. Y. Acad. Sci. 1125 (2008) 137–146.

[151] P.L. Tremblay, T. Zhang, S.A. Dar, C. Leang, D.R. Lovley, The Rnf complex of *Clostridium ljungdahlii* is a proton-translocating ferredoxin:NAD$^+$ oxidoreductase essential for autotrophic growth, mBio 4 (2012) e00406–e00412.

[152] H. Seedorf, W.F. Fricke, B. Veith, H. Brüggemann, H. Liesegang, A. Strittmatter, M. Miethke, W. Buckel, J. Hinderberger, F. Li, C. Hagemeier, R.K. Thauer, G. Gottschalk, The genome of *Clostridium kluyveri*, a strict anaerobe with unique metabolic features, Proc. Natl. Acad. Sci. U. S. A. 105 (2008) 2128–2133.

[153] P. Worm, A.J. Stams, X. Cheng, C.M. Plugge, Growth- and substrate-dependent transcription of formate dehydrogenase and hydrogenase coding genes in *Syntrophobacter fumaroxidans* and *Methanospirillum hungatei*, Microbiology 157 (2011) 280–289.

[154] I.A. Pereira, A.R. Ramos, F. Grein, M.C. Marques, S.M. da Silva, S.S. Venceslau, A comparative genomic analysis of energy metabolism in sulfate reducing bacteria and archaea, Front. Microbiol. 2 (2011) 69.

[155] E. Biegel, S. Schmidt, J.M. Gonzalez, V. Müller, Biochemistry evolution and physiological function of the Rnf complex, a novel ion-motive electron transport complex in prokaryotes, Cell. Mol. Life Sci. 68 (2011) 613–634.

[156] M.J. McInerney, L. Rohlin, H. Mouttaki, U. Kim, R.S. Krupp, L. Rios-Hernandez, J. Sieber, C.G. Struchtemeyer, A. Bhattacharyya, J.W. Campbell, R.P. Gunsalus, The genome of *Syntrophus aciditrophicus*: life at the thermodynamic limit of microbial growth, Proc. Natl. Acad. Sci. U. S. A. 104 (2007) 7600–7605.

[157] H. Kumagai, T. Fujiwara, H. Matsubara, K. Saeki, Membrane localization, topology, and mutual stabilization of the *rnfABC* gene products in *Rhodobacter capsulatus* and implications for a new family of energy-coupling NADH oxidoreductases, Biochemistry 36 (1997) 5509–55021.

[158] J. Steuber, Na$^+$ translocation by bacterial NADH:quinone oxidoreductases: an extension to the complex-I family of primary redox pumps, Biochim. Biophys. Acta 1505 (2001) 45–56.

[159] A. Saaf, M. Johansson, E. Wallin, G. von Heijne, Divergent evolution of membrane protein topology: the *Escherichia coli* RnfA and RnfE homologues, Proc. Natl. Acad. Sci. U. S. A. 96 (1999) 8540–8544.

[160] J. Backiel, O. Juárez, D.V. Zagorevski, Z. Wang, M.J. Nilges, B. Barquera, Covalent binding of flavins to RnfG and RnfD in the Rnf complex from *Vibrio cholerae*, Biochemistry 47 (2008) 11273–11284.

[161] M. Punta, P.C. Coggill, R.Y. Eberhardt, J. Mistry, J. Tate, C. Boursnell, N. Pang, K. Forslund, G. Ceric, J. Clements, A. Heger, L. Holm, E.L. Sonnhammer, S.R. Eddy, A. Bateman, R.D. Finn, The PFAM protein families database, Nucleic Acids Res. 40 (2012) D290–D301.

[162] Y. Jouanneau, H.S. Jeong, N. Hugo, C. Meyer, J.C. Willison, Overexpression in *Escherichia coli* of the *rnf* genes from *Rhodobacter capsulatus* —characterization of two membrane-bound iron–sulfur proteins, Eur. J. Biochem. 251 (1998) 54–64.

[163] T. Yagi, The bacterial energy-transducing NADH-quinone oxidoreductases, Biochim. Biophys. Acta 1141 (1993) 1–17.

[164] T. Yagi, T. Yano, A. Matsuno-Yagi, Characteristics of the energy-transducing NADH-quinone oxidoreductase of *Paracoccus denitrificans* as revealed by biochemical, biophysical, and molecular biological approaches, J. Bioenerg. Biomembr. 25 (1993) 339–345.

[165] S. Malki, I. Saimmaime, G. De Luca, M. Rousset, Z. Dermoun, J.P. Belaich, Characterization of an operon encoding an NADP-reducing hydrogenase in *Desulfovibrio fructosovorans*, J. Bacteriol. 177 (1995) 2628–2636.

[166] O. Schmitz, G. Boison, R. Hilscher, B. Hundeshagen, W. Zimmer, F. Lottspeich, H. Bothe, Molecular biological analysis of a bidirectional hydrogenase from cyanobacteria, Eur. J. Biochem. 233 (1995) 266–276.

[167] A. Tran-Betcke, U. Warnecke, C. Böcker, C. Zaborosch, B. Friedrich, Cloning and nucleotide sequences of the genes for the subunits of NAD-reducing hydrogenase of *Alcaligenes eutrophus* H16, J. Bacteriol. 172 (1990) 2920–2929.

[168] I.M. Fearnley, J.E. Walker, Conservation of sequences of subunits of mitochondrial complex I and their relationships with other proteins, Biochim. Biophys. Acta 1140 (1992) 105–134.

[169] J.E. Walker, The NADH:ubiquinone oxidoreductase (complex I) of respiratory chains, Q. Rev. Biophys. 25 (1992) 253–324.

[170] H.J. Abken, U. Deppenmeier, Purification and properties of an $F_{420}H_2$ dehydrogenase from *Methanosarcina mazei* Gö1, FEMS Microbiol. Lett. 154 (1997) 231–237.

[171] L.A. Sazanov, P. Hinchliffe, Structure of the hydrophilic domain of respiratory complex I from *Thermus thermophilus*, Science 311 (2006) 1430–1436.

[172] Y. Wang, L.Y. Geer, C. Chappey, J.A. Kans, S.H. Bryant, Cn3D: sequence and structure views for Entrez, Trends Biochem. Sci. 25 (2000) 300–302.

[173] M. Kallberg, H.P. Wang, S. Wang, J. Peng, Z.Y. Wang, H. Lu, J.B. Xu, Template-based protein structure modeling using the RaptorX web server, Nat. Protoc. 7 (2012) 1511–1522.

[174] S. Halboth, A. Klein, *Methanococcus voltae* harbors four gene clusters potentially encoding two [NiFe] and two [NiFeSe] hydrogenases, each of the cofactor F_{420}-reducing or F_{420}-non-reducing types, Mol. Gen. Genet. 233 (1992) 217–224.

[175] D.J. Mills, S. Vitt, M. Strauss, S. Shima, J. Vonck, *De novo* modeling of the F_{420}-reducing [NiFe]-hydrogenase from a methanogenic archaeon by cryo-electron microscopy, eLife 2 (2013) e00218.

[176] A. Dupuis, I. Prieur, J. Lunardi, Toward a characterization of the connecting module of complex I, J. Bioenerg. Biomembr. 33 (2001) 159–168.

[177] M. Sato, P.K. Sinha, J. Torres-Bacete, A. Matsuno-Yagi, T. Yagi, Energy transducing roles of antiporter-like subunits in *Escherichia coli* NDH-1 with main focus on subunit NuoN (ND2), J. Biol. Chem. 288 (2013) 24705–24716.

[178] M. Simianu, E. Murakami, J.M. Brewer, S.W. Ragsdale, Purification and properties of the heme- and iron–sulfur-containing heterodisulfide reductase from *Methanosarcina thermophila*, Biochemistry 37 (1998) 10027–10039.

[179] S. Heiden, R. Hedderich, E. Setzke, R.K. Thauer, Purification of a cytochrome *b* containing H$_2$:heterodisulfide oxidoreductase complex from membranes of *Methanosarcina barkeri*, Eur. J. Biochem. 213 (1993) 529–535.

[180] S. Heiden, R. Hedderich, E. Setzke, R.K. Thauer, Purification of a 2-subunit cytochrome *b* containing heterodisulfide reductase from methanol-grown *Methanosarcina barkeri*, Eur. J. Biochem. 221 (1994) 855–861.

[181] E. Murakami, U. Deppenmeier, S.W. Ragsdale, Characterization of the intramolecular electron transfer pathway from 2-hydroxyphenazine to the heterodisulfide reductase from *Methanosarcina thermophila*, J. Biol. Chem. 276 (2001) 2432–2439.

[182] R. Hedderich, N. Hamann, M. Bennati, Heterodisulfide reductase from methanogenic archaea: a new catalytic role for an iron–sulfur cluster, Biol. Chem. 386 (2005) 961–970.

[183] E.C. Duin, S. Madadi-Kahkesh, R. Hedderich, M.D. Clay, M.K. Johnson, Heterodisulfide reductase from *Methanothermobacter marburgensis* contains an active-site [4Fe-4S] cluster that is directly involved in mediating heterodisulfide reduction, FEBS Lett. 512 (2002) 263–268.

[184] A.M. Malinen, G.A. Belogurov, A.A. Baykov, R. Lahti, Na$^+$-pyrophosphatase: a novel primary sodium pump, Biochemistry 46 (2007) 8872–8878.

[185] S. Bäumer, S. Lentes, G. Gottschalk, U. Deppenmeier, Identification and analysis of proton-translocating pyrophosphatases in the methanogenic archaeon *Methanosarcina mazei*, Archaea 1 (2002) 1–7.

[186] V.N. Khmelenina, O.N. Rozova, Y.A. Trotsenko, Characterization of the recombinant pyrophosphate-dependent 6-phosphofructokinases from *Methylomicrobium alcaliphilum* 20Z and *Methylococcus capsulatus* Bath, Methods Enzymol. 495 (2011) 1–14.

[187] B. Tjaden, A. Plagens, C. Dörr, B. Siebers, R. Hensel, Phosphoenolpyruvate synthetase and pyruvate, phosphate dikinase of *Thermoproteus tenax*: key pieces in the puzzle of archaeal carbohydrate metabolism, Mol. Microbiol. 60 (2006) 287–298.

[188] J.M. Davies, R.J. Poole, P.A. Rea, D. Sanders, Potassium transport into plant vacuoles energized directly by a proton-pumping inorganic pyrophosphatase, Proc. Natl. Acad. Sci. U. S. A. 89 (1992) 11701–11705.

[189] T. Friedrich, K. Steinmüller, H. Weiss, The proton-pumping respiratory complex I of bacteria and mitochondria and its homolog in chloroplasts, FEBS Lett. 367 (1995) 107–111.

[190] H.L. Mi, T. Endo, T. Ogawa, K. Asada, Thylakoid membrane-bound, NADPH-specific pyridine-nucleotide dehydrogenase complex mediates cyclic electron-transport in the cyanobacterium *Synechocystis* sp. PCC-68038, Plant Cell Physiol. 36 (1995) 661–668.

[191] N. Battchikova, M. Eisenhut, E.M. Aro, Cyanobacterial NDH-1 complexes: novel insights and remaining puzzles, Biochim. Biophys. Acta 1807 (2011) 935–944.

[192] S. Bäumer, E. Murakami, J. Brodersen, G. Gottschalk, S.W. Ragsdale, U. Deppenmeier, The $F_{420}H_2$:heterodisulfide oxidoreductase system from *Methanosarcina* species. 2-Hydroxyphenazine mediates electron transfer from $F_{420}H_2$ dehydrogenase to heterodisulfide reductase, FEBS Lett. 428 (1998) 295–298.

[193] J. Kunow, D. Linder, K.O. Stetter, R.K. Thauer, $F_{420}H_2$:quinone oxidoreductase from *Archaeoglobus fulgidus* - characterization of a membrane-bound multisubunit complex containing FAD and iron–sulfur clusters, Eur. J. Biochem. 223 (1994) 503–511.

[194] H. Brüggemann, F. Falinski, U. Deppenmeier, Structure of the F420H2: quinone oxidoreductase of Archaeoglobus fulgidus —identification and overproduction of the F420H2-oxidizing subunit, Eur. J. Biochem. 267 (2000) 5810–5814.

[195] Y.J. Park, C.B. Yoo, S.Y. Choi, H.B. Lee, Purifications and characterizations of a ferredoxin and its related 2-oxoacid:ferredoxin oxidoreductase from the hyperthermophilic archaeon, *Sulfolobus solfataricus* P1, J. Biochem. Mol. Biol. 39 (2006) 46–54.

[196] P.L. Hagedoorn, T. Chen, I. Schröder, S.R. Piersma, S. de Vries, W.R. Hagen, Purification and characterization of the tungsten enzyme aldehyde:ferredoxin oxidoreductase from the hyperthermophilic denitrifier *Pyrobaculum aerophilum*, J. Biol. Inorg. Chem. 10 (2005) 259–269.

[197] A. Tersteegen, D. Linder, R.K. Thauer, R. Hedderich, Structures and functions of four anabolic 2-oxoacid oxidoreductases in *Methanobacterium thermoautotrophicum*, Eur. J. Biochem. 244 (1997) 862–868.

[198] L. Kerscher, D. Oesterhelt, Purification and properties of two 2-oxoacid:ferredoxin oxidoreductases from *Halobacterium halobium*, Eur. J. Biochem. 116 (1981) 587–594.

[199] H. Sakuraba, T. Ohshima, Novel energy metabolism in anaerobic hyperthermophilic archaea: a modified Embden–Meyerhof pathway, J. Biosci. Bioeng. 93 (2002) 441–448.

[200] A. Kletzin, M.W. Adams, Tungsten in biological systems, FEMS Microbiol. Rev. 18 (1996) 5–63.

[201] R. Roy, M.W. Adams, Characterization of a fourth tungsten-containing enzyme from the hyperthermophilic archaeon *Pyrococcus furiosus*, J. Bacteriol. 184 (2002) 6952–6956.

[202] F. Mayer, V. Müller, Adaptations of anaerobic archaea to life under extreme energy limitation, FEMS Microbiol. Rev. (2013), http://dx.doi.org/10.1111/1574-6976.12043.

[203] Z. Mladenovska, B.K. Ahring, Growth kinetics of thermophilic *Methanosarcina* spp. isolated from full-scale biogas plants treating animal manures, FEMS Microbiol. Ecol. 31 (2000) 225–229.

[204] Q.S. Jin, Energy conservation of anaerobic respiration, Am. J. Sci. 312 (2012) 573–628.